



Hydrogen in the natural gas distribution network: Preliminary analysis of gas release and dispersion behaviour

Prepared by the **Health and Safety Executive, DNV GL
Lander Consulting Limited, Progressive Energy Ltd, and
Northern Gas Networks Ltd**

RR1169 (2022)
Research Report

© Crown copyright 2022

Prepared 2020

First published 2022

You may reuse this information (not including logos) free of charge in any format or medium, under the terms of the Open Government Licence. To view the licence: visit the [National Archives Website](#), write to the Information Policy Team, The National Archives, Kew, London TW9 4DU, or email psi@nationalarchives.gsi.gov.uk.

Some images and illustrations may not be owned by the Crown so cannot be reproduced without permission of the copyright owner. Enquiries should be sent to copyright@hse.gov.uk.

Hydrogen has the potential to be used as part of decarbonising the future energy system. Hydrogen can be used as a fuel ‘vector’ to store and transport low-carbon energy. Several UK projects are investigating the potential use of the existing natural gas transmission and distribution network to transport either hydrogen, or blends of hydrogen and natural gas, from production or storage sites to domestic or commercial appliances such as boilers, cookers, fires and ranges. Mathematical modelling is important to inform risk assessments to ensure that levels of safety for the public are maintained.

This report describes preliminary mathematical modelling of potential leaks from gas network assets such as valves and pipes when hydrogen, or hydrogen blends, are transported or used. The research considers the potential impact of leak rates and the dispersion behaviour of the gas. It uses published information from laboratory-scale experiments. The report presents a preliminary modelling case study to show how this potential impact might affect a commonly-used UK gas industry leak tightness testing procedure.

This research will be of interest to risk assessment specialists in the gas industry.

This report and the work it describes were funded by: the Health and Safety Executive (HSE); and the Office of Gas and Electricity Markets (Ofgem) via the Network Innovation Competition projects ‘H21’ and ‘HyDeploy2’. Its contents, including any opinions and/or conclusions expressed, are those of the authors alone and do not necessarily reflect HSE policy. including any opinions and/or conclusions expressed, are those of the authors alone and do not necessarily reflect HSE policy.

Hydrogen in the natural gas distribution network: Preliminary analysis of gas release and dispersion behaviour

Simon Gant¹, Ann Halford², Graham Atkinson¹, Adrian Kelsey¹, David Torrado¹, Phil Hooker¹, Dave Lander³, Thomas Isaac⁴, Russ Oxley⁵, Andrew Garrison¹, Richard Goff¹, Catherine Spriggs¹

1. Health and Safety Executive

Harpur Hill, Buxton, Derbyshire, SK17 9JN

2. DNV GL

Holywell Way, Loughborough, LE11 3UZ

3. Lander Consulting Limited

94 Sudeley, Dosthill, Tamworth, Staffordshire, B77 1JU

4. Progressive Energy Ltd

Swan House Bonds Mill, Bristol Rd, Stonehouse, GL10 3RF

5. Northern Gas Networks Ltd

Thorpe Business Park, 1100 Century Way, Colton, Leeds, LS15 8TU

ACKNOWLEDGEMENTS

The authors would like to thank Professors Wolfgang Rodi (Karlsruhe Institute of Technology) and Vladimir Molkov (Ulster University) for useful discussions, and Barbara Lowesmith for help in providing copies of the NaturalHy reports. The assistance of ASME, Elsevier and RAND Corporation is gratefully acknowledged for providing permission to reprint the figures in the Appendix.

HSE would also like to thank Jean-Marc Lacombe and Benjamin Truchot (INERIS¹) for undertaking an independent review of this work prior to publication.

¹ Institut National de l'Environnement Industriel et des Risques, www.ineris.fr, accessed 28 April 2020

KEY MESSAGES

Hydrogen has the potential to be used as part of decarbonising the future energy system. Hydrogen can be used as a fuel ‘vector’ to store and transport low-carbon energy.

Several UK projects are investigating the potential use of the existing natural gas transmission and distribution network to transport either hydrogen, or blends of hydrogen and natural gas, from production or storage sites to domestic or commercial appliances, such as boilers, cookers, fires and ranges. Mathematical modelling is important to inform risk assessments to ensure that levels of safety for the public are maintained.

This report describes preliminary mathematical modelling of potential leaks from gas network assets such as valves and pipes when hydrogen, or hydrogen blends are transported or used. The research considers the potential impact of leak rates and the dispersion behaviour of the gas. It uses published information from laboratory-scale experiments.

A modelling case study is presented to show how this might affect a commonly-used UK gas industry procedure for leak tightness testing. This research will be of interest to risk assessment specialists in the gas industry.

EXECUTIVE SUMMARY

There is currently significant interest in the UK in using hydrogen both in existing natural gas appliances and new hydrogen-ready appliances within residential, commercial and industrial buildings as a means of reducing carbon dioxide emissions and meeting climate-change targets. Several ongoing projects are investigating the feasibility of supplying hydrogen to properties using either the existing natural gas distribution network or a new purpose-built gas network.

Risk assessment is an important aspect of these projects. As part of the GB Gas Safety (Management) Regulations 1996, it must be demonstrated that changes to the gas quality do not prejudice the end users. To assess the risks when transitioning to low carbon gases, such as hydrogen, it is necessary to understand the likelihood of gas releases occurring and their consequences. This includes assessing leak rates, gas dispersion behaviour, ignition potential and the fire and explosion hazards.

This report presents a preliminary analysis of leak rates and dispersion behaviour of hydrogen-methane blends (with up to 100% hydrogen) using established empirical correlations taken from the literature. Fundamental properties of hydrogen and hydrogen-methane blends are first presented. The ratio of hydrogen to methane leak rates is then calculated across a range of pressures, using equations for laminar, turbulent, subsonic and choked flow. The analysis shows that for laminar leaks there is no significant increase in the volumetric flow rate when adding up to 70% hydrogen, due to the viscosity remaining practically unchanged. For blends with more than 70% hydrogen, the volumetric flow rate increases up to 1.23 times the methane value (for 100% hydrogen). Subsonic and choked releases are shown to behave similarly to incompressible turbulent releases and produce volumetric flows rates that increase continuously, at a rising rate, as the percentage of hydrogen is increased, up to 2.8 times for 100% hydrogen as compared to the equivalent methane volumetric flow rate.

The resulting behaviour of turbulent jets and buoyant plumes in air is then assessed in terms of the change in extent of the flammable cloud for hydrogen blends as compared to methane. For jets, it is shown that the flammable cloud extends 3.5 times further for 100% hydrogen than for methane. For buoyancy-dominated plumes, the difference between hydrogen blends and methane is less significant.

A model for gas accumulation in an enclosure with upper and lower ventilation openings is then presented and applied to study the gas tightness testing aspects of the Institute of Gas Engineers and Managers IGE/UP/1 procedure. Results from the analysis suggest that gas installations that have been leak tested in accordance with IGE/UP/1 should have no increase in risk of producing flammable clouds if the gas is switched from natural gas to a blend of 20% or 50% hydrogen in natural gas. However, the method used by IGE/UP/1 to define the Maximum Permitted Leak Rate (MPLR) for different gases in terms of energy content would lead to an increased risk of producing flammable clouds for hydrogen blends. It was shown that a possible solution to this issue could be to define the MPLR for hydrogen blends and 100% hydrogen to be the same as the current MPLR for natural gas in terms of volumetric flow rate instead of energy. The gas accumulation model predicts practically identical gas concentrations in terms of percentage LEL for pure methane, hydrogen blends and 100% hydrogen in that case.

CONTENTS

1	INTRODUCTION	8
2	GAS PROPERTIES	9
3	RELEASE RATES	12
3.1	Laminar flow	12
3.2	Turbulent flow	15
3.3	Subsonic flow	16
3.4	Choked flow	16
4	DISPERSION	19
4.1	Jets	19
4.2	Intermediate jet-plume	22
4.3	Plumes	22
4.4	When do jets become plumes?	23
4.5	Quadvent-2 software comparison	25
4.6	Gas accumulation	27
5	EXAMPLE APPLICATION TO IGE/UP/1	28
6	CONCLUSIONS	35
7	REFERENCES	36
	Appendix A	39

1 INTRODUCTION

There are several large-scale projects ongoing in the UK that are assessing the feasibility of supplying hydrogen to residential, commercial and industrial buildings. The H21 project² is focussed on repurposing the existing gas distribution network, whilst the H100 project³ is proposing a new purpose-built network – in both cases for transporting 100% hydrogen. As part of the HyDeploy project⁴, a trial is currently being undertaken at Keele University where a blend of 20% hydrogen in natural gas is being supplied to properties across the campus. The UK Government Department for Business, Energy and Industrial Strategy (BEIS) is also funding research under the Hy4Heat programme⁵ on developing new hydrogen appliances, gas quality criteria and meters.

Risk assessment is an important aspect of these projects. As part of the GB Gas Safety (Management) Regulations 1996 (GSMR, 1996), it must be demonstrated that changes to the gas quality do not prejudice the end users. To assess the risks posed by the change in gas composition, it is necessary to understand the likelihood of gas releases occurring and their consequences. This includes assessing leak rates, gas dispersion behaviour, ignition potential and the fire and explosion hazards.

The aim of this report is to address two fundamental questions relating to leak rates and dispersion behaviour:

- For a given hole size, does hydrogen leak more than natural gas? If so, by how much?
- What is its effect on the size of the flammable cloud?

The gas pressures of interest span the range from domestic supply pressures of around 21 mbarg to the operating pressure of the UK National Transmission System (NTS) of around 85 barg. This preliminary study is focused on above-ground leaks, rather than those from buried assets, although some of the models discussed here are relevant to both cases.

The approach taken to answering these questions has been to use established empirical correlations taken from the literature and build upon previous work undertaken by others. The report starts by presenting the fundamental properties of hydrogen and hydrogen-blends. The ratio of hydrogen to natural gas leak rates is then calculated across a range of pressures, using equations for laminar, turbulent, subsonic and choked flow. The resulting behaviour of free jets and buoyant plumes in air is then assessed in terms of the change in extent of the flammable cloud for hydrogen (and hydrogen blends) as compared to methane. Finally, the UK Institute of Gas Engineers and Managers utilization procedure IGE/UP/1 is analysed to assess its implications for hydrogen. Throughout the report, to simplify the analysis, methane has been used as a substitute for natural gas.

² <http://www.h21.green>, accessed 25 November 2019.

³ <https://sgn.co.uk/about-us/future-of-gas/hydrogen/hydrogen-100>, accessed 25 November 2019.

⁴ <https://hydeploy.co.uk/>, accessed 25 November 2019.

⁵ <https://hy4heat.info>, accessed 25 November, 2019.

2 GAS PROPERTIES

The primary gas properties relevant to release and dispersion behaviour are the density, viscosity, specific heat capacity and flammable limits. Pure hydrogen has a molecular mass of $M_{H_2} = 2.016$ g/mol and is therefore around 14 times lighter than air at the same temperature and pressure. In comparison, methane has a molecular mass $M_{CH_4} = 16.043$ g/mol, and has a density just over half that of air. The density of gas mixtures is calculated from the volume-fraction weighted sum of the component gases, as shown in Figure 1a.

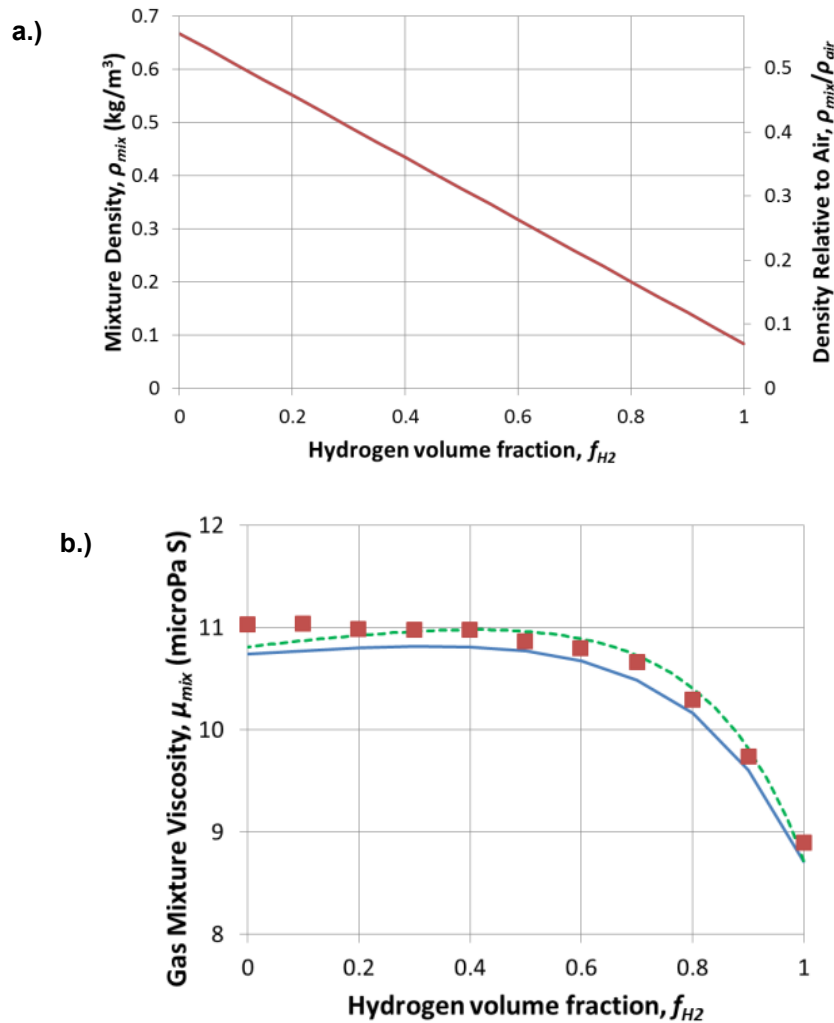


Figure 1 a.) Density of hydrogen-methane blends (top); b.) Viscosity of hydrogen-methane blends: ■ measurements by Kobayashi *et al.* (2007), — Davidson (1993) model predictions, --- GasVLe model predictions (bottom).

Several methods have been proposed in the literature for calculating the viscosity of gas mixtures (Kreiger, 1951; Brokaw, 1968; Davidson 1993). The present work is based on the “simple and accurate” method presented in the US Bureau of Mines report by Davidson (1993), which takes as inputs the molecular masses and viscosities of the constituent gases. The model was coded into a spreadsheet and

verified by comparing results to the helium-neon mixtures presented in the Davidson (1993) report⁶. It was then used to predict the measurements of Kobayashi *et al.* (2007) for hydrogen-methane blends and gave good agreement with the data (Figure 1b)⁷. Predictions from the GasVLe software⁸ using the Wilke-Brokaw formula with the Dean-Stiel density correction (see Reid *et al.*, 1977) are also shown in Figure 1b for comparison purposes. It is worth noting that the gas mixture viscosity does not decrease linearly from the methane viscosity to the hydrogen viscosity as the volume fraction of hydrogen is increased. Instead, the mixture viscosity remains nearly constant up to a hydrogen volume fraction of 70% v/v before decreasing to the hydrogen value.

Coward and Jones (1952) reported that the flammability limits of hydrogen-methane mixtures could be calculated fairly well using Le Chatelier's law (see Figure 2a). The flammable limit values used here for pure methane and hydrogen are taken from Coward and Jones (1952) and Zabetakis (1965), who gave the lower and upper limits for methane as 5.0% v/v and 15% v/v, and those for hydrogen as 4.0% v/v and 75% v/v. Other sources in the literature provide slightly different values. For example, the British Standard on explosive atmospheres, BS EN 80079-20-1 (BSI, 2019), quotes the lower and upper flammability limits for methane as 4.4% v/v and 17% v/v. These flammability limit values are all measured for upward-propagating flames in flame tubes. Higher concentrations of 9.0% v/v are needed to sustain downward-propagating flames of hydrogen. A detailed discussion of the characteristics of upward and downward propagating flames, together with data from several experimental tests, was presented by Coward and Jones (1952).

The ratio of the specific heat capacities ($\gamma = c_p/c_v$) is used to calculate the speed of sound in compressible gas mixtures and in formulae for choked and subsonic release rates (presented later in this report). The values of γ for pure methane and hydrogen are fairly similar (1.31 for methane and 1.41 for hydrogen at 15°C and 101,325 Pa)⁹. To determine the value of γ for methane-hydrogen mixtures, the specific heat capacities (c_p and c_v , in kJ/kg K) are calculated for methane-hydrogen mixtures from their mass-fraction weighted averages, and then γ is found from the ratio of these values. Results are presented in Figure 2b for three pressures (standard atmospheric pressure, 7 barg and 85 barg).

⁶ It appears that there may be a mistake in the units of viscosity presented in the Davidson (1993) report. For example, the pure helium dynamic viscosity is presented as 194 $\mu\text{Pa}\cdot\text{s}$ (or $1.94 \times 10^{-4} \text{Pa}\cdot\text{s}$), whereas the value given by the AirLiquide encyclopedia (<https://encyclopedia.airliquide.com>) is 1.94×10^{-4} Poise. Since 1 Poise is equivalent to 0.1 Pa·s, this equates to $1.94 \times 10^{-5} \text{Pa}\cdot\text{s}$. Using the same viscosities as Davidson (1993), it was possible to reproduce the gas mixture viscosity graphs presented in his US Bureau of Mines report, which was taken as sufficient verification of the model for the purposes of the present work.

⁷ The Kobayashi *et al.* (2007) measurements were taken at a temperature of 20 °C. Predictions from the Davidson (1993) model use pure component viscosities from <https://encyclopedia.airliquide.com> at the nearest temperature of 15 °C. GasVLe results are also for 15 °C.

⁸ <https://www.dnvgl.com/services/gasvle-8331>, accessed 14 January 2020.

⁹ Source: <https://encyclopedia.airliquide.com>, accessed 14 November 2019.

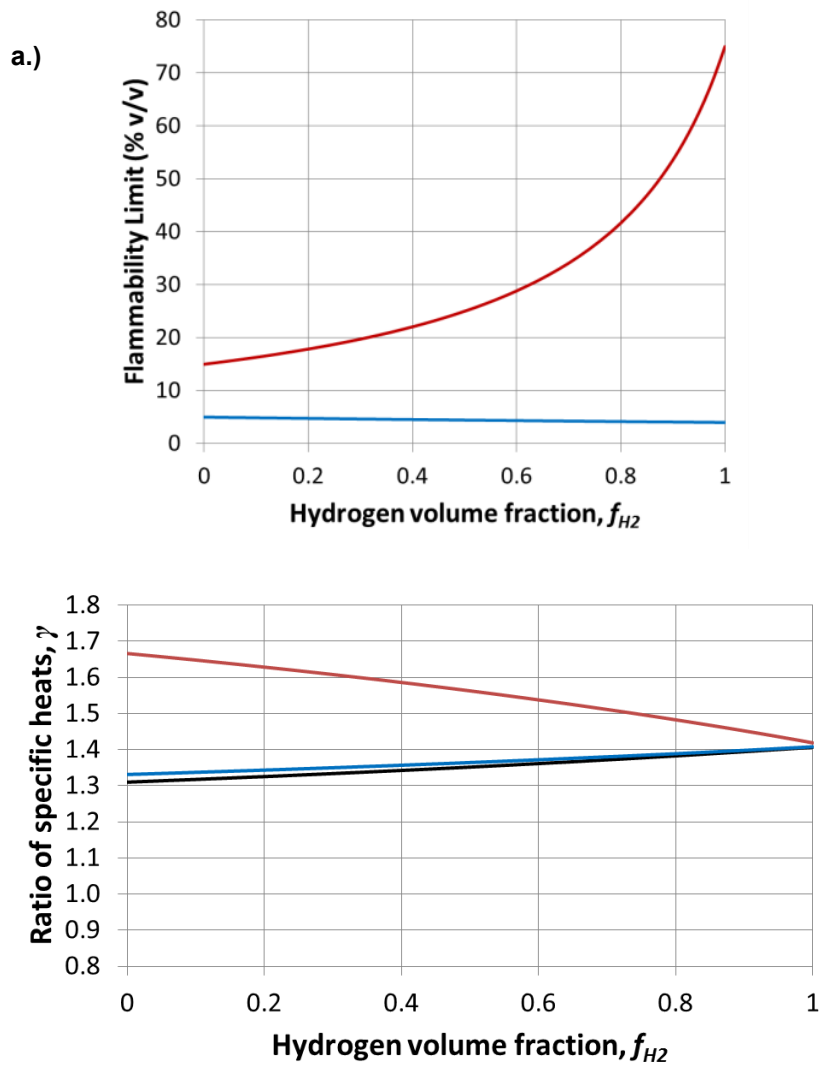


Figure 2 a.) Flammability limits calculated using Le Chatelier's law, — lower, — upper (top);
 b.) Ratio of specific heat capacities ($\gamma = c_p / c_v$) at three different pressures: — standard atmospheric pressure, — 7 barg, — 85 barg (bottom)

3 RELEASE RATES

Leaks of gas from pressurized pipes and vessels can occur in several different flow regimes. In order of increasing velocity and/or hole size these are: laminar flow, turbulent flow (incompressible), subsonic flow (compressible and turbulent) and choked flow (sonic, compressible and turbulent). These are considered below and for each regime the release rate of hydrogen relative to the release rate of methane is calculated.

3.1 LAMINAR FLOW

Laminar flow occurs at low speeds through small holes, producing smooth flow paths and little mixing. The dimensionless quantity that is used to characterise when laminar flow occurs is the Reynolds number, Re , defined as:

$$Re = \frac{\rho U D}{\mu} \quad (1)$$

where ρ is the density, U is the velocity, μ is the dynamic viscosity and D is the characteristic length (e.g. diameter of the hole through which the flow is passing). Laminar flow is produced in pipes below Reynolds numbers of around 2,000 (Massey, 1990). At higher Reynolds numbers of between 2,000 and 4,000 a transition occurs and for Reynolds numbers above 4,000 the flow is usually turbulent.

Swain and Swain (1992) examined the ratio of hydrogen to methane flow rates for laminar flow using Darcy's equation for the volumetric flow rate, $\dot{V}_{laminar}$:

$$\dot{V}_{laminar} = \frac{\Delta P \pi D^4}{128 L \mu} \quad (2)$$

where ΔP is the pressure drop between the inside of the pipe (or vessel) and the atmosphere, and L is the length of the hole. For the same supply pressure and temperature, and the same hole shape and size, they showed that the volumetric leak rate of hydrogen relative to methane is given by the ratio of the dynamic viscosities of the two gases:

$$\frac{\dot{V}_{H_2}}{\dot{V}_{CH_4}} = \frac{\mu_{CH_4}}{\mu_{H_2}} = \frac{1.1 \times 10^{-5}}{8.7 \times 10^{-6}} = 1.23 \quad (3)$$

This can be converted into a mass flow rate using the formula:

$$\frac{\dot{m}_{H_2}}{\dot{m}_{CH_4}} = \frac{M_{H_2}}{M_{CH_4}} \frac{\dot{V}_{H_2}}{\dot{V}_{CH_4}} = \frac{2}{16} 1.23 = 0.15 \quad (4)$$

The ratio of hydrogen to methane release rates can also be expressed in terms energy (or heat) fluxes of the two gases, using the heats of combustion ($Q_{H_2} = 285.8$ MJ/kmol; $Q_{CH_4} = 890.8$ MJ/kmol; CRC, 2008):

$$\frac{\dot{Q}_{H_2}}{\dot{Q}_{CH_4}} = \frac{Q_{H_2}}{Q_{CH_4}} \frac{\dot{V}_{H_2}}{\dot{V}_{CH_4}} = \frac{285.8}{890.8} 1.23 = 0.40 \quad (5)$$

The "gross" heats of combustion are used above, meaning that water produced in the combustion reaction is condensed into liquid, and the heat of combustion value accounts for the resulting release of latent heat. "Net" heats of combustion are sometimes quoted in the literature, for which the water in the combustion products is assumed to remain in the vapour state. The gross value is around 5% to 10% higher than the net heat of combustion for hydrocarbon gases such as methane, and around 15% higher than the net value

for hydrogen. To calculate the heat released in a fire, it is more appropriate to use the net value, since water remains as vapour in that case. In addition, when assessing the heat load from thermal radiation from fires, it is necessary to take into account the combustion efficiency and radiative heat fraction. Such analysis is left to future work.

Further results are shown in Figure 3 for hydrogen-methane blends. The viscosity of the blended gas in these plots was found using the Davidson (1993) model presented earlier. A notable feature of the right-hand plot is that the volumetric flow rate of blended gas remains virtually the same as that of pure methane up to a hydrogen volume fraction of 70% v/v, due to the fact that the viscosity of the blended gas is similar to that of pure methane (see Figure 1b). This has important implications for projects like HyDeploy, which involve gas blends with 20% v/v hydrogen.

To gain some practical appreciation for when laminar flow occurs in leaking assets, it is possible to rearrange the expression for the volumetric flow rate (Equation 2) and the Reynolds number (Equation 1), to find the limiting (maximum) hole diameter for which the flow remains laminar:

$$D_{limit} = \left(\frac{32 L Re \mu^2}{\Delta P \rho} \right)^{\frac{1}{3}} \quad (6)$$

Figure 4 presents two plots showing the behaviour of this equation for pure methane and pure hydrogen. The left-hand plot shows the limiting hole size for laminar flow as a function of pressure from 20 mbarg to 80 mbarg, assuming a path length of 5 mm. These values are relevant for leaks on above-ground assets in the Low Pressure (LP) natural gas network where the wall thickness is around 5 mm (e.g. the H21 above-ground leakage tests with cast-iron assets). The results show that hydrogen produces laminar flow in larger holes than methane. The right-hand graph in Figure 4 shows the limiting diameter for laminar flow as a function of path length for a pressure drop of 21 mbar. This is relevant to leaks from gas fittings and pipework at domestic supply pressures. For a flow path length of 1 mm (approximately the wall thickness of a gas pipe in a domestic setting), hydrogen gives laminar flow in holes up to 0.3 mm in diameter, as compared to holes up to 0.17 mm diameter for methane.

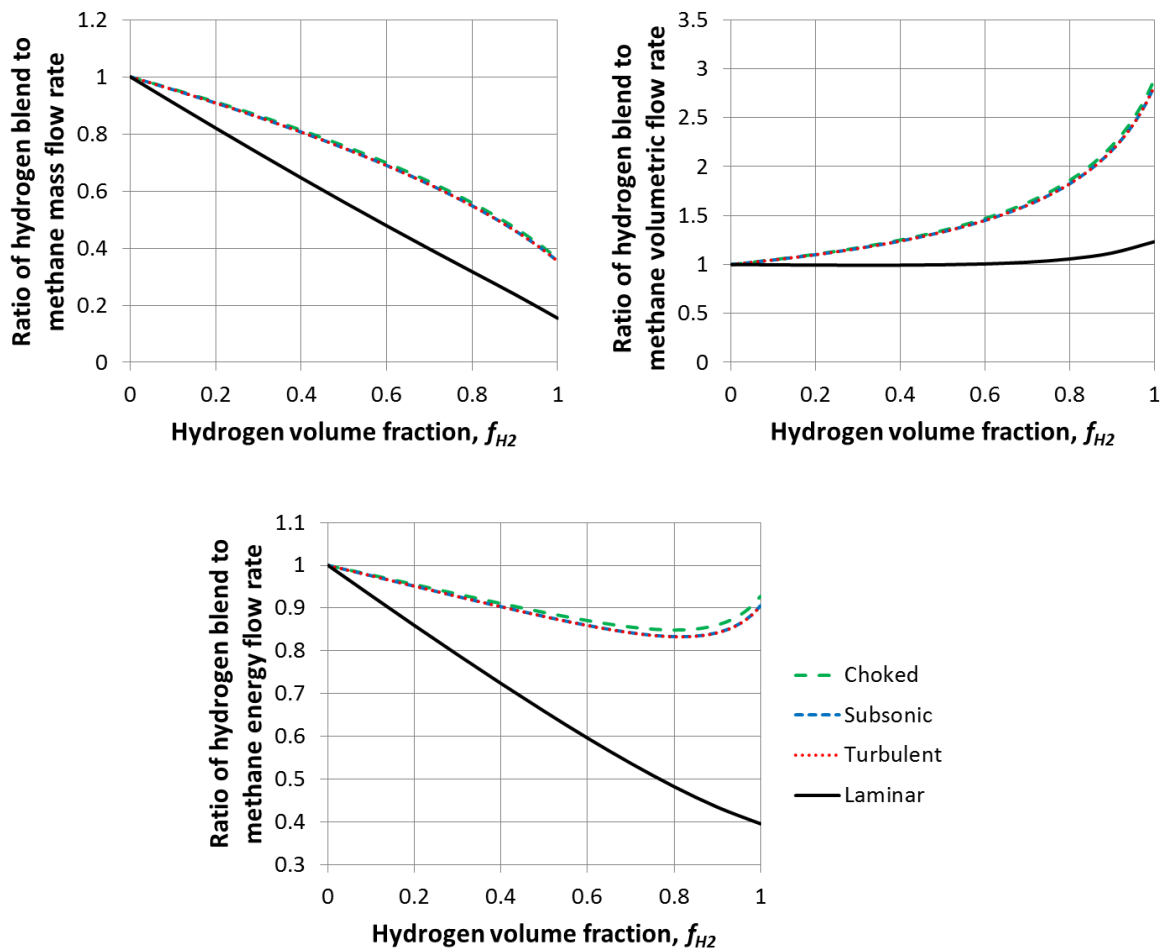


Figure 3 Ratio of hydrogen-methane blend to pure methane releases rates for choked, subsonic, turbulent and laminar flows in terms of the mass flux (left), volume flux (right) and energy flux (bottom).

Swain and Swain (1992) tested ten leaks in domestic gas pipes using methane, hydrogen and propane. Four leaks were fabricated by modifying home gas pipe fittings to simulate errors made during installation. The remaining six leaks involved gas pipes/fittings provided by a local (American) gas pipe company that had been removed from service due to excessive leakage rates. The holes in the first three tests were semi-circular in cross-section with diameters of 0.18 mm, 0.42 mm and 0.71 mm. Swain and Swain (1992) found that the majority of the leaks produced flow rates that indicated the flow was laminar at typical operating gas pressures.

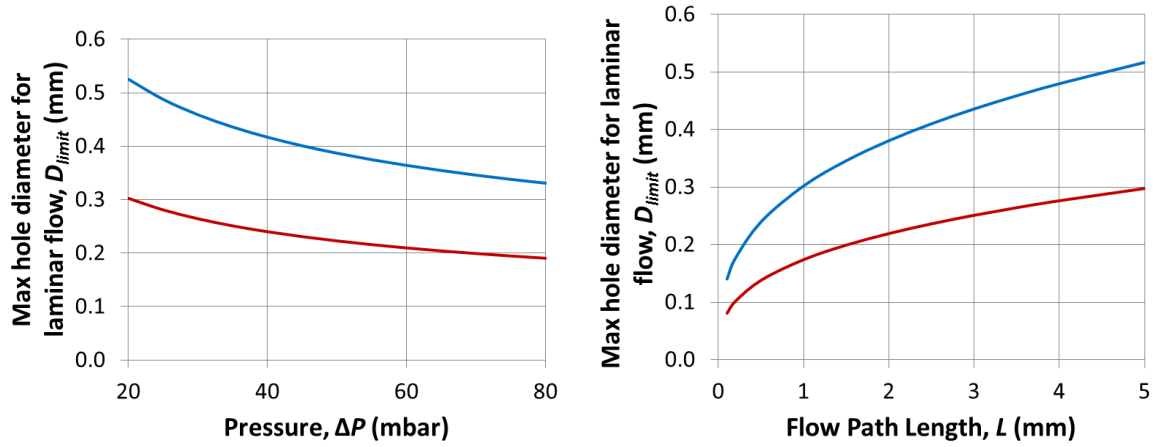


Figure 4 Maximum limiting hole diameters for laminar flow: — hydrogen, — methane. The left-hand plot assumes a flow path length of 5 mm, and the right-hand plot assumes a pressure of 21 mbar.

3.2 TURBULENT FLOW

Swain and Swain (1992) also analysed the ratio of hydrogen to methane leak rates for turbulent flow, where they modelled the volumetric flow rate using Darcy's equation, as follows:

$$\dot{V}_{turbulent} = 0.354\pi \frac{D^{2.5}\sqrt{\Delta P}}{\sqrt{fL\rho}} \quad (7)$$

where f is the friction factor, which is assumed to be constant for turbulent flow. Using this equation, they showed that the ratio of hydrogen to methane volumetric flow rates is equal to the inverse of the square-root of the gas densities (assuming that the hydrogen and methane leaks are through the same hole, at the same release temperature and pressure):

$$\frac{\dot{V}_{H_2}}{\dot{V}_{CH_4}} = \sqrt{\frac{\rho_{CH_4}}{\rho_{H_2}}} = \sqrt{\frac{M_{CH_4}}{M_{H_2}}} = \sqrt{\frac{16}{2}} = 2.8 \quad (8)$$

This result can be converted into mass and energy flow rates as before. The resulting ratio of the hydrogen to methane release rates in terms of mass is 0.35 and in terms of energy is 0.91. Results are presented in Figure 3 for hydrogen-methane blends. The hockey-stick shape to the energy release rate curve with a minima at a hydrogen volume fraction of around 0.8 is a consequence of combining the volumetric flow rate ratio (the curve sweeping upwards shown in Figure 3) with the heat of combustion of the hydrogen blend (a straight line that decreases linearly from the pure methane value of 890.8 MJ/kmol to the hydrogen value of 285.8 MJ/kmol as the hydrogen volume fraction increases from 0 to 1).

3.3 SUBSONIC FLOW

In the analysis presented by Swain and Swain (1992), gas-compressibility effects were not taken into account. This assumption is appropriate for low gas pressures (e.g. domestic gas pressures of 21 mbarg) but it may produce errors at higher pressures.

The critical pressure, P_c , is calculated as follows:

$$P_c = P_{atm} \left(\frac{2}{\gamma + 1} \right)^{-\gamma/(\gamma-1)} \quad (9)$$

where P_{atm} is the atmospheric pressure and γ is the ratio of specific heats. The critical pressure, P_c , is 0.85 barg for pure methane and 0.91 barg for pure hydrogen. For pressures below the critical pressure, the flow is subsonic (not choked) and the mass flow rate of a compressible ideal gas can be calculated as follows (BSI, 2015):

$$\dot{m} = C_d A P \sqrt{\frac{M}{ZRT} \frac{2\gamma}{(\gamma-1)} \left[1 - \left(\frac{P_{atm}}{P} \right)^{(\gamma-1)/\gamma} \right] \left(\frac{P_{atm}}{P} \right)^{1/\gamma}} \quad (10)$$

where C_d is the discharge coefficient, A is the cross-sectional area of the opening, P is the pressure inside the vessel or pipe, R is the universal gas constant (8,314 J kmol⁻¹ K⁻¹) and Z is the compressibility correction factor, which takes a value of 1.0 for ideal gases.

Using this equation, the ratio of hydrogen to methane mass release rates is:

$$\frac{\dot{m}_{H_2}}{\dot{m}_{CH_4}} = C_{subsonic} \sqrt{\frac{M_{H_2}}{M_{CH_4}}} = \begin{cases} 1.000 \sqrt{\frac{2}{16}} = 0.35 & \text{for } P = 21 \text{ mbarg} \\ 1.026 \sqrt{\frac{2}{16}} = 0.36 & \text{for } P = 0.9 \text{ barg} \end{cases} \quad (11)$$

where $C_{subsonic}$ contains the terms dependent upon pressure and the ratio of specific heats. This varies between bounding values of $C_{subsonic} = 1.0$ to 1.026 across the range of pressures from 21 mbarg to 0.9 barg, which gives ratios of hydrogen to methane mass flow rates of between 0.35 and 0.36, i.e. practically identical values to the value obtained previously for turbulent flow. In terms of volumetric flow rates (using Equation 4) the ratios are between 2.8 and 2.9, and in terms of energy flow rates (using Equation 5) the ratios are between 0.91 and 0.93. Results are presented in Figure 3 for hydrogen blends at a pressure of 21 mbarg. The plots show that subsonic releases exhibit practically the same behaviour as turbulent releases.

3.4 CHOKED FLOW

Choked flow is a limiting condition reached when the pressure in the pipe or vessel is above the critical pressure, P_c . The velocity of the gas at the orifice in this case is sonic (i.e. a Mach number of one). If the pressure is increased still higher, above P_c , the velocity of gas at the orifice remains fixed at the speed of sound, but the mass flow rate increases due to an increase in the density of the gas. In the UK gas distribution network, there are three pressure tiers: Low Pressure (LP) from 19 mbarg to 75 mbarg, Medium Pressure (MP) from 75 mbarg to 2 barg and Intermediate Pressure (IP) from 2 to 7 barg. Choked

flow is therefore only relevant for leaks from MP and IP assets. Gas pressures in domestic properties are typically around 21 mbarg, and therefore leaks within homes will not behave as choked releases.

When the flow is choked, the mass flow rate is given by the following equation (BSI, 2015):

$$\dot{m} = C_d A P \sqrt{\gamma \frac{M}{ZRT} \left(\frac{2}{\gamma + 1} \right)^{(\gamma+1)/(\gamma-1)}} \quad (12)$$

For the same leak conditions (i.e. the same hole size, discharge coefficient, pressure and temperature), the ratio of the hydrogen to methane mass flow rates is then:

$$\frac{\dot{m}_{H_2}}{\dot{m}_{CH_4}} = C_{choked} \sqrt{\frac{M_{H_2}}{M_{CH_4}}} = 1.025 \sqrt{\frac{2}{16}} = 0.36 \quad (13)$$

The term C_{choked} in the above equation is a function of γ and is equal to 1.025 for the ratio of hydrogen to methane. The resulting ratio of mass flow rates is 0.36, which is practically the same as the value obtained previously for subsonic releases. In terms of volumetric flow rates, (using Equation 4) the ratio is 2.9, and in terms of energy flow rates (using Equation 5) the ratio is 0.93. Results for hydrogen blends are presented in Figure 3, and they show very similar behaviour to that obtained previously for turbulent and subsonic releases.

The expansion of a compressible gas from a pressurized vessel or pipe to atmospheric pressure causes a reduction in the gas temperature (and hence an increase in the gas density). This decrease in temperature is a function of the ratio of specific heat capacities of the gas. For subsonic releases, the relevant equation for the density at the source is given in BS EN 60079-10-1 (BSI, 2015), and for choked releases, the following expression is given by Ewan and Moodie (1986):

$$\rho_0 = \rho_g \left(\frac{\gamma + 1}{2} \right) \quad (14)$$

where ρ_0 is the gas density at the source and ρ_g is the gas density at the upstream (stagnation) temperature in the vessel or pipe. Since γ is different for hydrogen and methane, the degree of cooling is different for the two gases. The results presented in Figure 3 do not take into account this difference in temperature, and instead the conversion from mass to volumetric flow rates has simply used the ratio of the molecular masses (as in Equation 4), which assumes that the hydrogen and methane temperatures are the same. Calculations have been performed which factor in the different densities given by the equation in BS EN 60079-10-1 and Equation 14, and the effect is very small. For both subsonic and choked releases, the resulting error in the ratio of hydrogen to methane volume flow rates is a maximum of 4% in relative terms (i.e. a change in the ratio $\dot{V}_{H_2}/\dot{V}_{CH_4}$ from 2.9 to 2.8).

Before concluding this section, it is worth noting that for turbulent, subsonic or choked releases, the above analysis has shown that the ratio of hydrogen to methane release rates can be estimated quickly (with an error of less than a few percent) from the square-root of the ratio of the molecular masses of the two gases, i.e.:

$$\frac{\dot{m}_{H_2}}{\dot{m}_{CH_4}} \approx \sqrt{\frac{M_{H_2}}{M_{CH_4}}} \quad ; \quad \frac{\dot{V}_{H_2}}{\dot{V}_{CH_4}} \approx \sqrt{\frac{M_{CH_4}}{M_{H_2}}} \quad (15)$$

The ratio of hydrogen to methane release rates is given by a single set of curves shown in Figure 3. In future work, it would be useful to revisit this analysis using realistic natural gas compositions. Properties such as the ratio of specific heat capacities may differ, particularly at high pressures.

4 DISPERSION

4.1 JETS

Chen and Rodi (1980) provided the following expression for the decay of concentration with distance in vertical buoyant jets issuing from a round orifice:

$$y = k \left(\frac{\rho_0}{\rho_a} \right)^{\frac{1}{2}} \frac{D}{x} \quad (16)$$

where y is the concentration expressed as a mass fraction, k is a model constant, ρ_0 and ρ_a are the source gas density and ambient (air) density, D is the source diameter and x is the distance downstream from the source. A notable feature of this equation is that the concentration does not depend on the release velocity. Instead, the concentration at a given distance only depends on the source gas density and the diameter of the source. This behaviour is related to the entrainment of fresh air into the jet. Air entrainment rates are proportional to the centreline velocity of the jet (Ricou and Spalding, 1961). A faster jet releases more gas, but it also entrains air at a faster rate and these two effects balance each other out. Different values for the constant k are proposed in the literature, which may relate to different initial conditions (George, 1989) and a value of 5.4 from Chen and Rodi (1980) is often used. The dependence of concentration on the ratio (ρ_a/ρ_0) originates from the work of Ricou and Spalding (1961) who studied the entrainment of air into jets of air, hydrogen, propane and carbon dioxide. The fact that their work included hydrogen jets lends some support to the analysis presented here. Further background to Chen and Rodi's work is provided in the Appendix.

Equation 16 can be rearranged in terms of the distance x to the LFL concentration. The expression can then be used to assess the change in the distance to the LFL for hydrogen relative to methane, as follows:

$$\frac{x_{H2}}{x_{CH4}} = \left(\frac{\rho_{H2}}{\rho_{CH4}} \right)^{\frac{1}{2}} \frac{y_{CH4}}{y_{H2}} = \left(\frac{M_{H2}}{M_{CH4}} \right)^{\frac{1}{2}} \frac{y_{CH4}}{y_{H2}} = \left(\frac{2}{16} \right)^{\frac{1}{2}} \frac{2.8}{0.29} = 3.5 \quad (17)$$

where the LFL mass fractions for hydrogen and methane are $y_{H2} = 0.29\%$ w/w and $y_{CH4} = 2.8\%$ w/w. The above result shows that flammable hydrogen clouds will extend 3.5 times further than the equivalent flammable methane clouds in situations where there is a free unobstructed vertical jet release from the same round hole, at the same temperature and pressure. The result is insensitive to the pressure of the release, provided it is below the critical pressure (i.e. below around 0.85 barg).

The fact that flammable hydrogen jets are larger than the equivalent methane jets is not related to the fact that the release rate of hydrogen is 2.8 times greater than methane (for a turbulent release). As noted earlier, the release rate does not feature in the relevant equation for gas concentration (Equation 16). Instead, the larger flammable cloud for hydrogen is caused by the significant difference in density between the gas and the surrounding air. The jet momentum is reduced quickly in hydrogen jets, since the air density is so much higher than the hydrogen density. This loss in momentum means that air is entrained at a slower rate into hydrogen jets than into methane jets. Since less air is entrained, hydrogen jets dilute more slowly and gas concentrations remain above the LFL for longer, giving a larger distance to the LFL.

Above the critical pressure, gas releases are choked. The flow immediately downstream of the orifice features a series of expansion waves and shocks as the jet expands to reach atmospheric pressure. The behaviour of the jet downstream of the shocks resembles a subsonic jet produced by a larger source than the actual orifice. Models for this scenario using "pseudo" or "equivalent" source conditions have been developed by Birch *et al.* (1984, 1987) and Ewan and Moodie (1986) (see Molkov, 2015, for a recent

review and Ruffin *et al.*, 1996, for further validation). Their models can be written in the following form for the mass fraction along the centreline of the jet:

$$y = k \left(\frac{\rho_0}{\rho_a} \right)^{\frac{1}{2}} \frac{D_{eff}}{x + a} \quad (18)$$

where D_{eff} is the effective diameter of the jet pseudo-source, and a is an offset distance from the orifice to the “virtual” origin of the jet. Birch *et al.* (1984, 1987) derived their equation for concentration in terms of the volume fraction, not mass fraction, but their equation can be converted into the above form, as shown in the Appendix. Birch *et al.* (1987) provided the following expression for the effective diameter, D_{eff} :

$$\frac{D_{eff}}{D} = C_D \sqrt{\left[\frac{P}{P_{atm}} \left(\frac{2}{\gamma + 1} \right)^{\frac{1}{\gamma-1}} \frac{\gamma}{(\gamma C_D^2 + 1)} \right]} \quad (19)$$

where C_D is the discharge coefficient, P is the upstream pressure in the pipe or vessel and P_{atm} is the atmospheric pressure¹⁰. Birch *et al.* (1987) assumed a discharge coefficient of 1.0 and they also found that the concentration offset distance, a , was independent of the pressure and equal to 0.6 orifice diameters. This offset distance is small in comparison to the length of the flammable cloud and therefore in the analysis presented here it is ignored. Their model also assumed that the temperature of the gas at the pseudo-source is the same as the temperature of gas in the pipe or vessel (i.e. the density ρ_0 in Equation 18 is evaluated at the upstream temperature in the pipe or vessel).

It is possible to rearrange Equations 18 and 19 to express the distance, x , to a particular mass fraction, y , and from there derive the following equation for the distance to the LFL for hydrogen relative to methane for a choked release:

$$\frac{x_{H2}}{x_{CH4}} = \left(\frac{M_{H2}}{M_{CH4}} \right)^{\frac{1}{2}} \frac{y_{CH4}}{y_{H2}} \frac{f(\gamma_{H2})}{f(\gamma_{CH4})} = \left(\frac{2}{16} \right)^{\frac{1}{2}} \frac{2.8}{0.29} 1.02 = 3.5 \quad (20)$$

The function $f(\gamma)$ in the above equation is the term on the right-hand side of Equation 19, without the pressures, which cancel since it is assumed the methane and hydrogen releases are from pipes or vessels at the same pressure. The ratio of specific heats changes relatively little between hydrogen and methane, and therefore the ratio of the two functions of hydrogen to methane, $f(\gamma_{H2})/f(\gamma_{CH4})$, is close to one. The analysis predicts that the distance to the LFL is 3.5 times larger for hydrogen than for methane, which is practically identical to the result obtained earlier for subsonic releases.

Ewan and Moodie (1986) used a different expression for the effective pseudo-source diameter, as follows:

$$\frac{D_{eff}}{D} = \left(\frac{P_e}{P_a} \right)^{\frac{1}{2}} \quad ; \quad P_e = P \left(\frac{2}{\gamma + 1} \right)^{\frac{\gamma}{\gamma-1}} \quad (21)$$

where P_e is the exit pressure at the orifice. Their model assumed that the temperature of the gas at the pseudo-source was cooler than the upstream pressure due to expansion of the gas, and their equation for the resulting density of the gas was given earlier (Equation 14). Equations 14, 18 and 21 can be rearranged into the following expression for the ratio of the hydrogen to the methane distance to LFL:

¹⁰ Birch *et al.* (1987) appear to have made two typographical errors in their paper when presenting this equation. Firstly the equals sign = was written as +. Secondly, the γ on the numerator of the final term was written as 1.

$$\frac{x_{H_2}}{x_{CH_4}} = \left[\frac{M_{H_2} (\gamma_{H_2} + 1)}{M_{CH_4} (\gamma_{CH_4} + 1)} \right]^{\frac{1}{2}} \frac{y_{CH_4}}{y_{H_2}} \left(\frac{2}{\gamma_{H_2} + 1} \right)^{\frac{\gamma_{H_2}}{\gamma_{H_2} - 1}} \left(\frac{2}{\gamma_{CH_4} + 1} \right)^{-\frac{\gamma_{CH_4}}{\gamma_{CH_4} - 1}} = 3.4 \quad (22)$$

Inserting appropriate values for M and γ into the above expression gives the result that the distance to the LFL for hydrogen is 3.4 times that of methane, i.e. similar to the values obtained previously using the Birch *et al.* (1987) pseudo-source for choked releases, and for the Chen and Rodi (1980) correlation for subsonic releases.

The values quoted above are based on evaluating γ at a pressure of 7 barg and a temperature of 15 °C. If, alternatively, it is evaluated at a higher pressure of 85 barg, the values of γ for hydrogen and methane change slightly (see Figure 2b). Equation 20 then gives a ratio (x_{H_2} / x_{CH_4}) of 3.3 and Equation 22 gives a ratio of 3.6.

The distance to a concentration of 50% LFL is often used instead of 100% LFL in area classification to take into account the fact that concentrations in jets and plumes fluctuate over time due to turbulence, and therefore concentrations at times exceed the predicted mean concentrations (Webber, 2002). The results presented above are for the distance to 100% LFL. Since the equations are expressed in terms of the ratio of the mass fractions (y_{CH_4}/y_{H_2}), and not the volume fractions, the results for the ratio of the distances (x_{H_2} / x_{CH_4}) are around 1% larger for 50% LFL (i.e. for the subsonic case, the ratio is 3.50 instead of 3.47). Figure 5 compares the ratio of predicted distances to the 50% LEL across the full range of hydrogen blends. The results show that choked releases behave similarly to subsonic releases across the range of gas compositions.

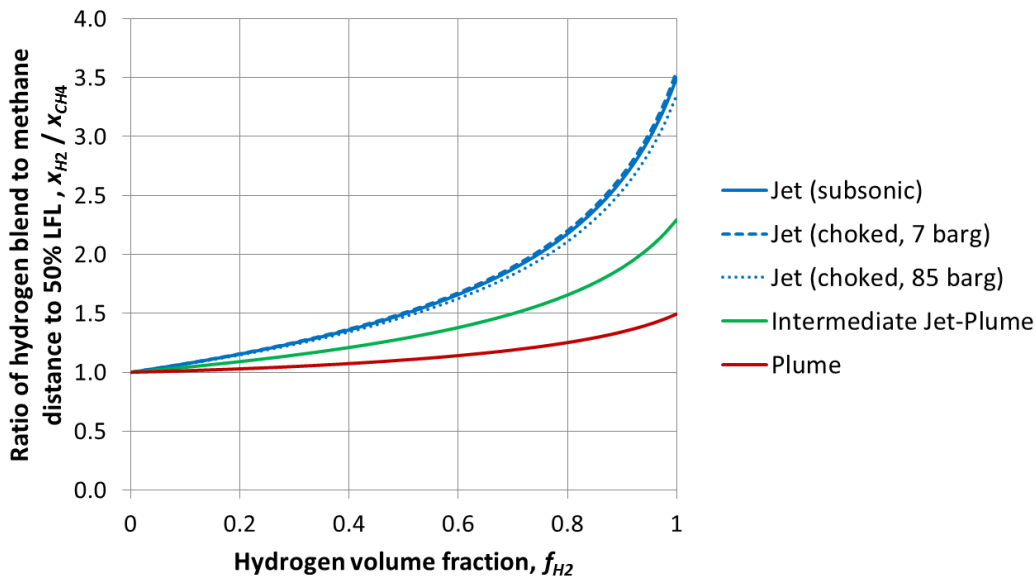


Figure 5 Ratio of the distance to 50% LFL for hydrogen blends relative to methane (x_{H_2}/x_{CH_4}) in free vertical turbulent round jets, plumes and intermediate jet-plumes. The results for the distance to 100% LFL are the same to two significant figures and appear nearly identical to those shown here for 50% LFL. The choked gas releases shown here are calculated using the Birch *et al.* (1987) pseudo-source but results are practically identical using the Ewan & Moodie (1986) model.

4.2 INTERMEDIATE JET-PLUME

Chen and Rodi (1980) also provided correlations for the decay of concentration in releases where buoyancy forces are more significant (i.e. where gas disperses more as a plume than a jet). For the intermediate regime between jet and plume, they gave the following correlation:

$$C^* = 4.4Fr^{\frac{1}{8}} \left(\frac{\rho_0}{\rho_a}\right)^{-\frac{7}{16}} \left(\frac{x}{D}\right)^{-\frac{5}{4}} \quad (23)$$

where C^* is the volume fraction (not the mass fraction as used earlier in the jet correlation – see Appendix) and the constant of 4.4 is taken from Smith *et al.* (1986)¹¹. The term Fr in the above equation is the Froude number, i.e. the ratio of inertial to buoyancy forces, which is calculated¹² from:

$$Fr = \frac{\rho_0 U_0^2}{gD(\rho_a - \rho_0)} \quad (24)$$

where U_0 is the release velocity and g is the acceleration due to gravity (9.81 m/s²). Following a similar approach to that used above for jets, the equation can be rearranged to express the ratio of the distance to the LFL for hydrogen relative to methane:

$$\begin{aligned} \frac{x_{H2}}{x_{CH4}} &= \left(\frac{C_{CH4}^*}{C_{H2}^*}\right)^{\frac{4}{5}} \left(\frac{U_{H2}}{U_{CH4}}\right)^{\frac{1}{5}} \left(\frac{M_{air} - M_{CH4}}{M_{air} - M_{H2}}\right)^{\frac{1}{10}} \left(\frac{M_{CH4}}{M_{H2}}\right)^{\frac{1}{4}} \\ &= \left(\frac{0.05}{0.04}\right)^{\frac{4}{5}} (2.8)^{\frac{1}{5}} \left(\frac{29 - 16}{29 - 2}\right)^{\frac{1}{10}} \left(\frac{16}{2}\right)^{\frac{1}{4}} = 2.3 \end{aligned} \quad (25)$$

In the above equation, the ratio of the hydrogen to methane initial velocities (U_{H2} / U_{CH4}) is 2.8 for turbulent releases (c.f. Equation 8 – assuming the hole size is the same for both the hydrogen and methane releases). The hydrogen and methane LFL volume fractions are taken to be $C_{H2}^* = 0.04$ v/v and $C_{CH4}^* = 0.05$ v/v (see Figure 2a). The equation shows that flammable hydrogen clouds will extend 2.3 times further than the equivalent flammable methane clouds in situations where the release is in the intermediate jet-plume regime. Further results for methane blends are presented in Figure 5.

4.3 PLUMES

Chen and Rodi (1980) gave the following correlation for the concentration decay along the centreline of vertical turbulent plumes, where the dispersion behaviour is dominated by buoyancy effects:

$$C^* = 9.35Fr^{\frac{1}{3}} \left(\frac{\rho_0}{\rho_a}\right)^{-\frac{1}{3}} \left(\frac{x}{D}\right)^{-\frac{5}{3}} \quad (26)$$

which can be rearranged as before to give:

¹¹ Chen and Rodi (1980) presented a different value of 0.44, which may have been a typographical mistake (for further discussion, see Gant *et al.*, 2011). In the analysis presented here, the constant cancels from the equation and therefore this ambiguity does not affect the findings.

¹² Other authors often define the Froude number as the square-root of the Froude number given here, as defined by Chen and Rodi (1980).

$$\frac{x_{H2}}{x_{CH4}} = \left(\frac{C_{CH4}^*}{C_{H2}^*}\right)^{\frac{3}{5}} \left(\frac{U_{H2}}{U_{CH4}}\right)^{\frac{2}{5}} \left(\frac{M_{air} - M_{CH4}}{M_{air} - M_{H2}}\right)^{\frac{1}{5}} = \left(\frac{5.0}{4.0}\right)^{\frac{3}{5}} (2.8)^{\frac{2}{5}} \left(\frac{29 - 16}{29 - 2}\right)^{\frac{1}{5}} = 1.5 \quad (27)$$

This shows that flammable hydrogen clouds will extend 1.5 times further than the equivalent flammable methane clouds in situations where the release is in the pure buoyancy-dominated plume regime.

4.4 WHEN DO JETS BECOME PLUMES?

Chen and Rodi (1980) presented the following parameter to determine the extent of the jet and plume regions:

$$B = Fr^{-\frac{1}{2}} \left(\frac{\rho_0}{\rho_a}\right)^{-\frac{1}{4}} \frac{x}{D} \quad (28)$$

where:

- $B < 0.5$ the flow is a momentum-dominated jet
- $0.5 < B < 5.0$ the flow is in an intermediate state between jet and plume
- $B > 5.0$ the flow is a buoyancy-dominated plume

From this equation, it can be seen that the transition from momentum-dominated (jet) to buoyancy-dominated (plume) behaviour occurs nearer the source if the density difference ($\rho_a - \rho_0$) is increased, the initial velocity (U_0) is decreased or the source diameter (D) is decreased.

Equation 28 can be combined with the equations presented earlier for jets and plumes, and rearranged to define the boundary between jet and plume behaviour at the point where the gas concentration reaches either 100% LFL or 50% LFL. Results from this analysis are presented in Figure 6 for methane and hydrogen in terms of the upstream pressure and hole size. The results show that hydrogen exhibits a greater tendency towards plume behaviour than methane, as expected from its lower density. The chevron shape to the three flow regions (jet, intermediate and plume) is due to the transition from subsonic to choked flow at the critical pressure (0.85 barg for methane and 0.91 barg for hydrogen). Below the critical pressure, when the release is subsonic, an increase in the pressure causes an increase in the release velocity and hence a higher Froude number (i.e. a greater tendency for the release to be jet-dominated). Above the critical pressure, when the release is choked, the velocity is capped at the speed of sound and an increase in the pressure produces a larger pseudo-source, which changes the behaviour. The Ewan and Moodie (1986) and Birch *et al.* (1987) models produce slightly different results when the flow is choked, as shown by the red and blue lines above the critical pressure. The coloured regions shown in the plot to distinguish between jet, intermediate and plume regions average between the results of these two choked-flow models.

The reason for producing Figure 6 is to help the reader assess which flow regime applies for their case of interest (in terms of pressure and hole size). This knowledge of the flow regime can then be used in conjunction with Figure 5 to identify how large a flammable cloud of hydrogen-blended gas will be produced, relative to the equivalent cloud of methane.

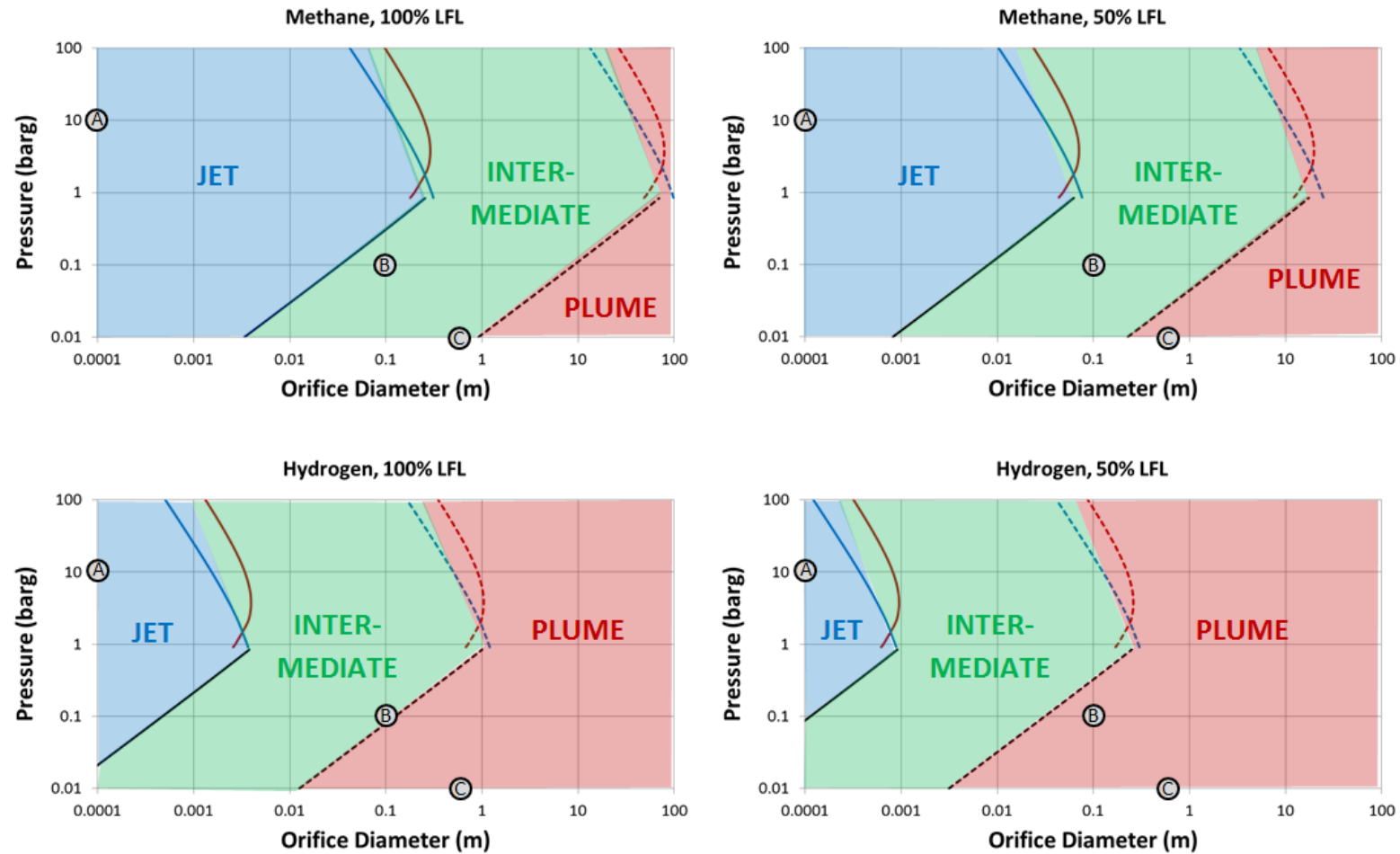


Figure 6 Jet, intermediate and plume regions for round buoyant jet releases of methane (top) and hydrogen (bottom) in air. Plots on the left are for the 100% LFL and on the right for 50% LFL. Lines mark the boundary between the regions. Solid lines are for the jet-to-intermediate boundary and broken lines for the intermediate-to-plume boundary. Line colours are: — subsonic, — choked (Ewan and Moodie, 1986), — choked (Birch *et al.*, 1987). Symbols marked A, B and C are three scenarios modelled in the Quadvent-2 software.

4.5 QUADVENT-2 SOFTWARE COMPARISON

As a check on the previous analysis, calculations were performed using the Quadvent-2 software¹³. This uses an integral-modelling approach to simulate the dispersion of jets and plumes, both in the open air or in ventilated rooms (Webber *et al.*, 2011, 2020). It uses the entrainment model of Ricou and Spalding (1961), but does not rely upon the empirical correlations presented by Chen and Rodi (1980). Three release conditions were simulated, shown in Figure 6 as circular symbols A, B and C, which were chosen to be in the jet, intermediate and plume flow regimes, respectively. Table 1 compares the results from Quadvent-2 to those predicted from the Chen and Rodi (1980) analysis presented above. In some cases, such as Condition B (an orifice diameter of 0.1 m and pressure of 0.1 barg), the hydrogen release is predicted to be in the plume regime whilst the methane release is in the intermediate jet-plume regime (at the point where the concentrations reach 50% LFL). The above analysis predicts that the ratio (x_{H_2} / x_{CH_4}) will be 1.5 in the former case and 2.3 in the latter, and so the Chen and Rodi (1980) result is presented in the table as a range between these values.

There is generally good agreement shown in Table 1 between the Quadvent-2 results and those obtained using the jet and plume correlations from Chen and Rodi (1980). For the jet release (Condition A), Quadvent-2 predicted the flammable hydrogen jet to extend 3.6 times further than the equivalent methane jet, and the Chen and Rodi analysis produces a value of 3.5. For the intermediate jet-plume case (Condition B), Quadvent-2 predicted values of (x_{H_2} / x_{CH_4}) to be 2.9 and 2.4 for the distance to 100% LFL and 50% LFL, respectively, whereas Chen and Rodi's correlations produced a value of 2.3 and a range between 2.3 (intermediate jet-plume) and 1.5 (plume). For the final plume case (Condition C), Quadvent-2 predicted (x_{H_2} / x_{CH_4}) values of 1.9 and 1.7, whilst the Chen and Rodi values were again in the range 2.3 to 1.5.

The benefit of the analysis in Sections 4.1 to 4.4 over Quadvent-2 is that it shows how the flammable cloud size is affected by the addition of hydrogen across the full range of conditions from zero to 100% hydrogen (see Figure 5). The correlations explain how the flow changes with hole size and pressure, rather than just providing spot values for certain scenarios. The dispersion behaviour is also characterised for the upper and lower bounding cases of momentum-driven jets and buoyancy-dominated plumes. In principle, these results could be obtained from Quadvent-2, but it would involve several hundred individual Quadvent-2 calculations to produce equivalent plots showing the trends in model behaviour.

The increase in the size of flammable clouds for hydrogen as compared to methane has been observed experimentally in work undertaken for the EMERGE project¹⁴ at the French laboratory, INERIS. Chaineaux and Schumann (1995) undertook experiments using a 5 m³ vessel that was initially pressurised to 40 bar and measured concentrations in free-jets of methane, propane and hydrogen using discharge orifices ranging from 25 mm to 150 mm in diameter. They found that the distance to LFL for hydrogen was around twice the distance for methane. The flammable cloud volume was also calculated to be approximately ten times larger for hydrogen.

¹³ <https://www.hsl.gov.uk/publications-and-products/quadvent-2>, accessed 24 September 2019.

¹⁴ *Extended Modelling and Experimental Research into Gas Explosions (EMERGE)*

Table 1 Comparison of Quadvent-2 predictions to the Chen and Rodi (1980) jet and plume correlations in terms of the ratio of the distances to LFL for hydrogen relative to methane (x_{H_2} / x_{CH_4})

	A: Jet	B: Intermediate Jet-Plume	C: Plume
Orifice diameter (m)	0.0001	0.1	0.5
Pressure (barg)	10	0.1	0.01
Release Rate (kg/s)			
Quadvent-2 Hydrogen (\dot{m}_{H_2})	5.5×10^{-6}	0.32	2.6
Quadvent-2 Methane (\dot{m}_{CH_4})	5.5×10^{-5}	0.90	7.2
Quadvent-2 ($\dot{m}_{H_2}/\dot{m}_{CH_4}$)	0.36	0.36	0.35
Predicted ($\dot{m}_{H_2}/\dot{m}_{CH_4}$), Equations 11 and 13	0.36	0.36	0.35
Distance to 100% LFL (m)			
Quadvent-2 Hydrogen (x_{H_2})	0.11	34	93
Quadvent-2 Methane (x_{CH_4})	0.030	12	49
Quadvent-2 (x_{H_2}/x_{CH_4})	3.6	2.9	1.9
Predicted (x_{H_2}/x_{CH_4}), Equations 20, 25 and 27	3.5	2.3	2.3 – 1.5
Distance to 50% LFL (m)			
Quadvent-2 Hydrogen (x_{H_2})	0.22	57	146
Quadvent-2 Methane (x_{CH_4})	0.062	23	84
Quadvent-2 (x_{H_2}/x_{CH_4})	3.6	2.4	1.7
Predicted (x_{H_2}/x_{CH_4}), Equations 20, 25 and 27	3.5	2.3 – 1.5	1.5

4.6 GAS ACCUMULATION

To investigate the build-up of gas in enclosed spaces, a modified version of the model developed by Lowesmith *et al.* (2009) has been investigated. This model simulates a jet release into a room and predicts the build-up over time of a stratified layer of buoyant gas near the ceiling. The enclosure has upper and lower ventilation openings in the walls through which gas and/or air can flow. In zero-wind conditions, the flow of air through the lower ventilation opening into the room is driven by the buoyancy of gas in the stratified layer, which forces itself out of the upper opening. The model was originally developed as part of the NaturalHy project by Lowesmith *et al.* (2009) and has been coded up independently by HSE. Further details of this work, which has been undertaken in support of the HyDeploy-2 project, will be published in due course.

The main modifications to the original Lowesmith *et al.* (2009) model by HSE consisted of simplifications to fix the height of the buoyant gas layer in the model, and to remove the jet sub-model. The modified model assumes that the gas is released at the mid-height of the enclosure and that it becomes fully-mixed in the upper half of the space (i.e. immediately above the release point). Lowesmith *et al.* used a turbulent jet model to predict the initial dilution of the gas, but in the present model this is not used and instead the concentration in the stratified layer is calculated from fully mixing the release rate of gas and the inflow of fresh air. These simplifications were made because the focus of the present work is to examine the gas tightness testing aspects of the IGE/UP/1 procedure (see below). The release rates are very low in this case (i.e. laminar) and it is necessary to consider small enclosures, such as metering boxes. It was considered inappropriate to use the turbulent jet model to simulate these small laminar releases. The modelling approach was guided by the British Gas work documented in the book by Harris (1983), which was based on an extensive programme of gas release experiments.

5 EXAMPLE APPLICATION TO IGE/UP/1

To illustrate how the work presented above can be applied in practice to the UK gas network, the IGE/UP/1 utilization procedure (IGEM, 2005) has been examined. The scope of this procedure is strength testing, tightness testing and direct purging of industrial and commercial gas installations. As part of the gas tightness testing process, the procedure introduces the concept of the Maximum Permitted Leak Rate (MPLR) of gas, which is the maximum flow rate of gas an installation is allowed to leak when the system is at the operating pressure. For new installations, the MPLR is defined on the basis of an energy release rate of 0.054 MJ/hr, which for natural gas equates to a volumetric flow rate of 0.0014 m³/hr. Different MPLR values are used for existing installations, depending upon the volume of the space enclosing the leak and the degree of ventilation.

Based on the work presented earlier in this report, the following questions are addressed:

1. Is a leak of gas at the MPLR laminar or turbulent?
2. For an installation with an existing natural gas leak equal to the MPLR, how would the leak rate change if the gas was switched to hydrogen (or a hydrogen-methane blend)? What would be the implications in terms of flammable cloud size?
3. The IGE/UP/1 procedure currently calculates the MPLR for different gases based on equivalent energy content (in MJ/hr). What would be the MPLR for hydrogen using this approach? What would be the implications in terms of the flammable cloud size?

To answer the first question: if the leak of gas is laminar, the flow rate will be governed by Equation 2, and if it is turbulent then the equations for turbulent or subsonic flow could be used (Equations 7 or 10). Using first the laminar flow equation, it is necessary to specify the length of the hole, L . Low pressure gas pipe wall thicknesses typically vary from 0.6 to 1.0 mm. The defect in the pipework/fittings producing the leak may not run straight through (perpendicular to) the pipe wall. Taking $L = 1$ mm as a starting point for the calculation, Equation 2 gives the equivalent hole size as 0.095 mm for a supply pressure of 21 mbarg. Assuming the gas in the pipework is at a temperature of 15 °C, the density of the methane at the orifice is $\rho_0 = 0.68$ kg/m³ and the dynamic viscosity¹⁵ of the gas is $\mu = 1.07 \times 10^{-5}$ Pa.s, the calculated Reynolds number (Equation 1) is around 330 (see Table 2), i.e. it is well below the transition Reynolds number of 2,000, which therefore indicates that the flow of methane is laminar. Figure 4 showed that if the gas is switched from methane to hydrogen and the flow is laminar for methane, then it will also be laminar for hydrogen. This analysis assumes that all of the gas leaks through a single, circular hole. If the gas leaks through a slot or through multiple smaller holes, then these too will be laminar since the characteristic dimension D in the Reynolds number (Equation 1) will be smaller.

Moving onto the second question, if the gas was switched from methane to hydrogen and the permitted hole size was unchanged (i.e. using the hole size calculated previously for methane of 0.095 mm), then it is possible to determine the flow rate of hydrogen blends using the laminar flow equation (Equation 2). For pure hydrogen, the volumetric flow is 1.23 times higher than the flow rate of methane, i.e. $1.23 \times 0.0014 = 0.0017$ m³/hr. The release rates for 20% and 50% hydrogen blends are unchanged (i.e. 0.0014 m³/hr). These release rates are summarised in Table 3 under the heading “Scenario I”.

¹⁵ Values taken from the Air Liquide online encyclopaedia: <https://encyclopedia.airliquide.com>, accessed 25 November 2019.

Table 2 IGE/UP/1 methane calculations for new installations and existing installations in Area Type A

- Methane MPLR volumetric flow rate = 0.0014 m³/hr
- Laminar flow calculation (Equation 2)
 - Methane MPLR hole diameter = 0.095 mm
 - Methane MPLR Reynolds number = 330
- Subsonic flow calculation (Equation 10)
 - Methane MPLR hole diameter = 0.080 mm
 - Methane MPLR Reynolds number = 395

To examine the implications of the change in flow rates on the flammable cloud size, the gas accumulation model discussed in Section 4.5 was used. The scenario modelled consisted of a leak into a small enclosure such as an internal cupboard housing a gas meter, with dimensions (height, width and depth) of 1.0 m, 1.0 m and 0.5 m, respectively. The cupboard was assumed to have no designed ventilation openings but have cracks around the top and bottom of the door, and these cracks were assumed to span the width of the cupboard (1.0 m). As a first step, calculations were performed assuming a crack width of 1 mm around the door (i.e. an opening area of 1.0 × 0.001 m, at the top and bottom of the cupboard). Results are presented in Figure 7 for the build-up over time of gas in the top half of the cupboard for four different gases: pure methane, two blends of 20% and 50% hydrogen in methane, and pure hydrogen. The results show that in all cases the concentrations are well below the LFL. The 20% and 50% hydrogen releases give practically identical concentrations (as a percentage of LFL) to pure methane. The release rates used in these calculations for the blended gases are given in Table 3.

Table 3 Hydrogen-blend calculations in support of IGE/UP/1

	Methane	20% Hydrogen	50% Hydrogen	100% Hydrogen
Relative molecular mass (kg/kmol)	16.043	13.2	9.0	2.016
Lower flammability limit (% v/v)	5.0	4.8	4.4	4.0
Gross heat of combustion (MJ/m ³)	37.7	32.6	24.9	12.1
Scenario I: Volumetric flow rate for the hole diameter calculated in Table 2 for the methane MPLR assuming laminar flow (m ³ /hr)	0.0014	0.0014	0.0014	0.0017
Scenario II: Volumetric flow rate that gives an energy flow rate of 0.054 MJ/hr (m ³ /hr)	0.0014	0.0017	0.0022	0.0045
Scenario III: Volumetric flow rate set equal to the current natural gas value of 0.0014 m ³ /hr	0.0014	0.0014	0.0014	0.0014

As a quick check on these calculations, Harris (1983) presented the following correlation for the minimum area of an opening needed to keep natural gas concentrations to “acceptable” levels in an enclosure:

$$A_b = \frac{1350\dot{V}_g}{\sqrt{H}} = \frac{1350 \left(\frac{0.0014}{3600} \right)}{\sqrt{1}} = 0.0005 \text{ m}^2 \quad (29)$$

where \dot{V}_g is the volume flow rate of gas and H is the vertical spacing between the upper and lower ventilation openings. The model assumes the flow is driven by the buoyancy of the gas and the openings are at the top and bottom of the enclosure. It predicts an opening area of 0.0005 m² for the MPLR flow rate of 0.0014 m³/hr, and if this area is distributed across the width of the enclosure, it equates to a crack width of 0.5 mm. The result therefore confirms the model calculations presented in Figure 7, i.e. that concentrations with a crack width of 1 mm should be well below the LFL.

The gas accumulation model was then used to simulate the same cupboard with a smaller 0.05 mm crack around the door, which was chosen to be sufficiently small to give concentrations close to the LFL. The results again showed that the concentrations remained below the LFL, with the 20% and 50% hydrogen cases again giving similar results to methane in terms of the percentage of LFL. For the pure hydrogen release, the steady state concentration was higher than the methane case. The results presented in Figure 7 imply that the risks of forming flammable clouds due to small leaks at or below the MPLR are the same for the 20% and 50% blends as they are for natural gas, which is an important finding in the context of the HyDeploy project.

To address the third question, the IGE/UP/1 methodology was used to calculate the flow rates of 20%, 50% and 100% hydrogen blends necessary to achieve an energy flow rate of 0.054 MJ/hr. These results are presented in Table 3, where they are referred to as Scenario II. Gas accumulation calculations were then performed for the same scenario of a gas leak in a 1.0 × 1.0 × 0.5 m cupboard considered previously and the results are presented in Figure 8 as dashed lines. For the cupboard with 1 mm wide openings, the

concentrations increased as the hydrogen content increased, but in all cases the steady-state concentrations were below the LFL. In the cupboard with a smaller crack width of 0.05 mm, the gas concentrations rose above the LFL for the 50% hydrogen blend and for the pure hydrogen release.

The results from this analysis suggest that the method used by IGE/UP/1 to define the MPLR for different gases would lead to an increased risk of producing flammable clouds for hydrogen blends. The low energy density of hydrogen per unit volume means that the MPLR volumetric flow rate is 3.1 times higher for pure hydrogen than it is for natural gas (0.0045 m³/hr versus 0.0014 m³/hr). In addition to the increased flow rate of gas, the LFL is also lower for hydrogen than natural gas, and the combined effects mean that hydrogen will be more likely to produce a flammable cloud than the current situation with natural gas.

A possible solution to this issue could be to define the MPLR for hydrogen blends and 100% hydrogen to be the same as the current MPLR for natural gas in volumetric terms, i.e. 0.0014 m³/hr for new installations or existing installations with Area Type A (insufficient ventilation). This is referred to as Scenario III in Table 3. Results are presented in Figure 9 for the 20%, 50% and 100% hydrogen blends with the leak rate in all cases of 0.0014 m³/hr. The gas accumulation model predicts practically identical results in terms of percentage LFL. In terms of gas concentration (in % v/v), the hydrogen blends produce lower concentrations than pure methane – i.e. the increase in buoyancy produces an increase in the ventilation rate, which dilutes the gas to a lower concentration. This is balanced by the lower LFL for the hydrogen blends so that, overall, the gas concentration as a percentage of LFL appears nearly identical for the four different gases.

This analysis has been performed assuming the pressure is the same for methane and hydrogen blends. In reality, there may be a greater drop in pressure along the pipework from the gas meter to equipment with hydrogen blends, due to the need to supply a higher volumetric flow rate of gas to the equipment for it to achieve the same heat output. This drop in pressure would only apply when the equipment was in operation, drawing gas along the pipe. Assuming that the pressure at the meter was the same for all gases, the effect of the higher pressure drop would be to reduce the leak rate for hydrogen blends. The result of analysis presented above should therefore be conservative, but it may be useful to investigate this matter further.

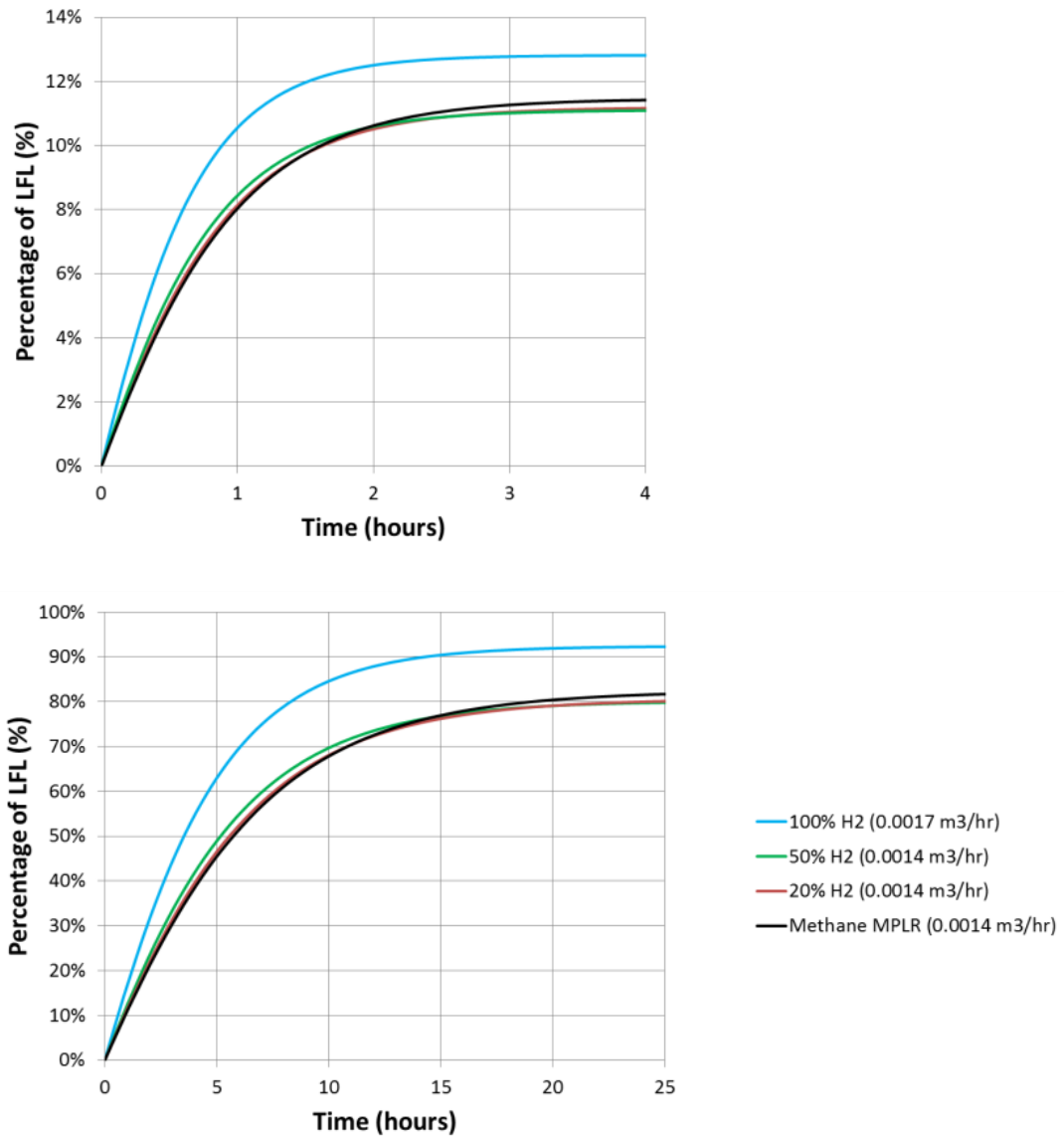


Figure 7 Predicted concentrations in a $1.0 \times 1.0 \times 0.5$ m enclosure with ventilation openings top and bottom that are 1.0 m across and have a width of either 1 mm (top) or 0.05 mm (bottom). Four gas compositions are tested, as given in Table 3. Solid lines used flow rates calculated with a hole diameter of 0.095 mm and pressure of 21 mbarg, which gives the MPLR flow rate of $0.0014 \text{ m}^3/\text{hr}$ for methane (Scenario I).

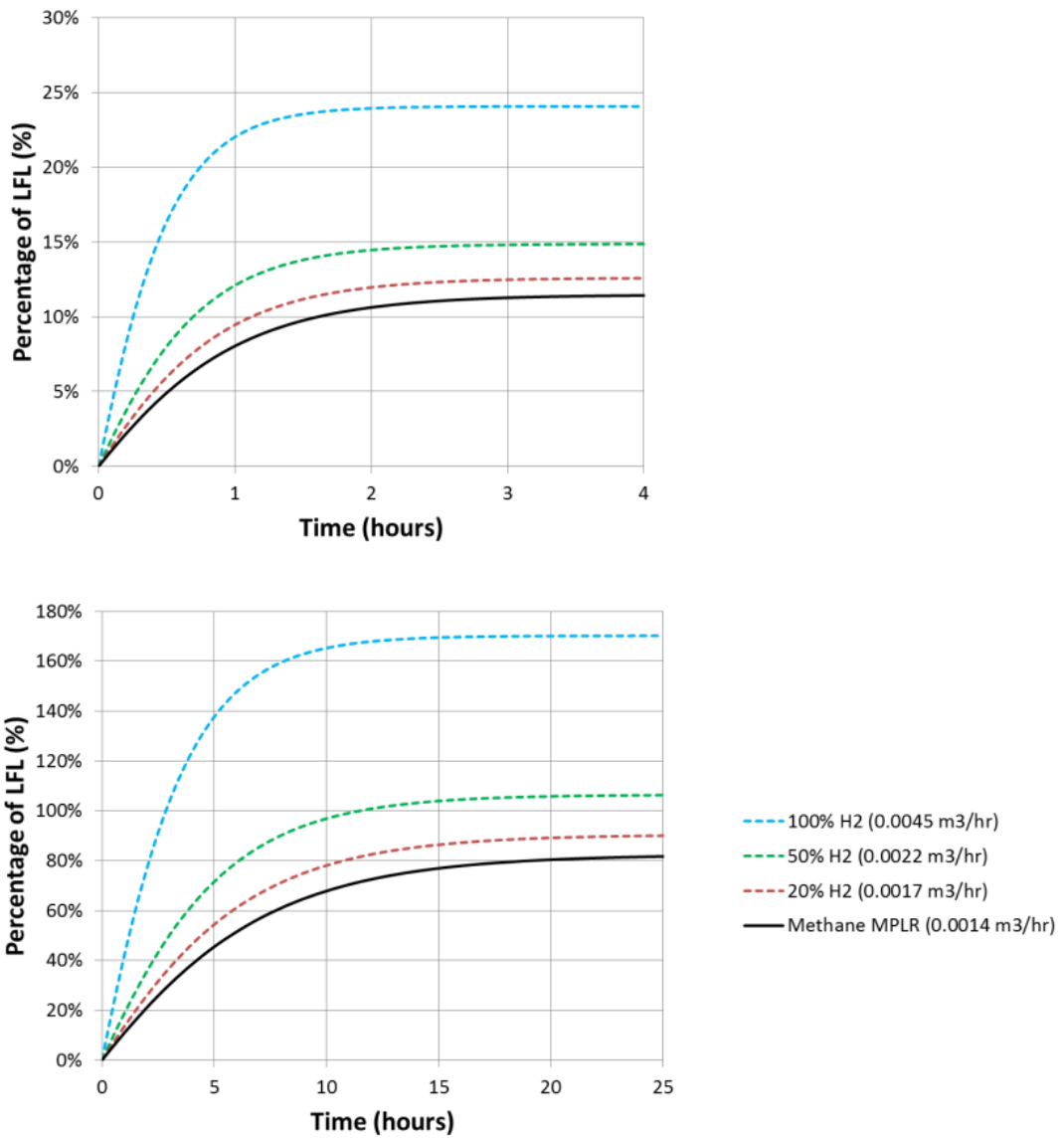


Figure 8 Predicted concentrations in a $1.0 \times 1.0 \times 0.5$ m enclosure with ventilation openings top and bottom that are 1.0 m across and have a width of either 1 mm (top) or 0.05 mm (bottom). Four gas compositions are tested, as given in Table 3. Dashed lines used flow rates calculated to give the energy flow rate of 0.054 MJ/hr specified in IGE/UP/1 (Scenario II). The solid black line is the result for the methane MPLR flow rate of $0.0014 \text{ m}^3/\text{hr}$.

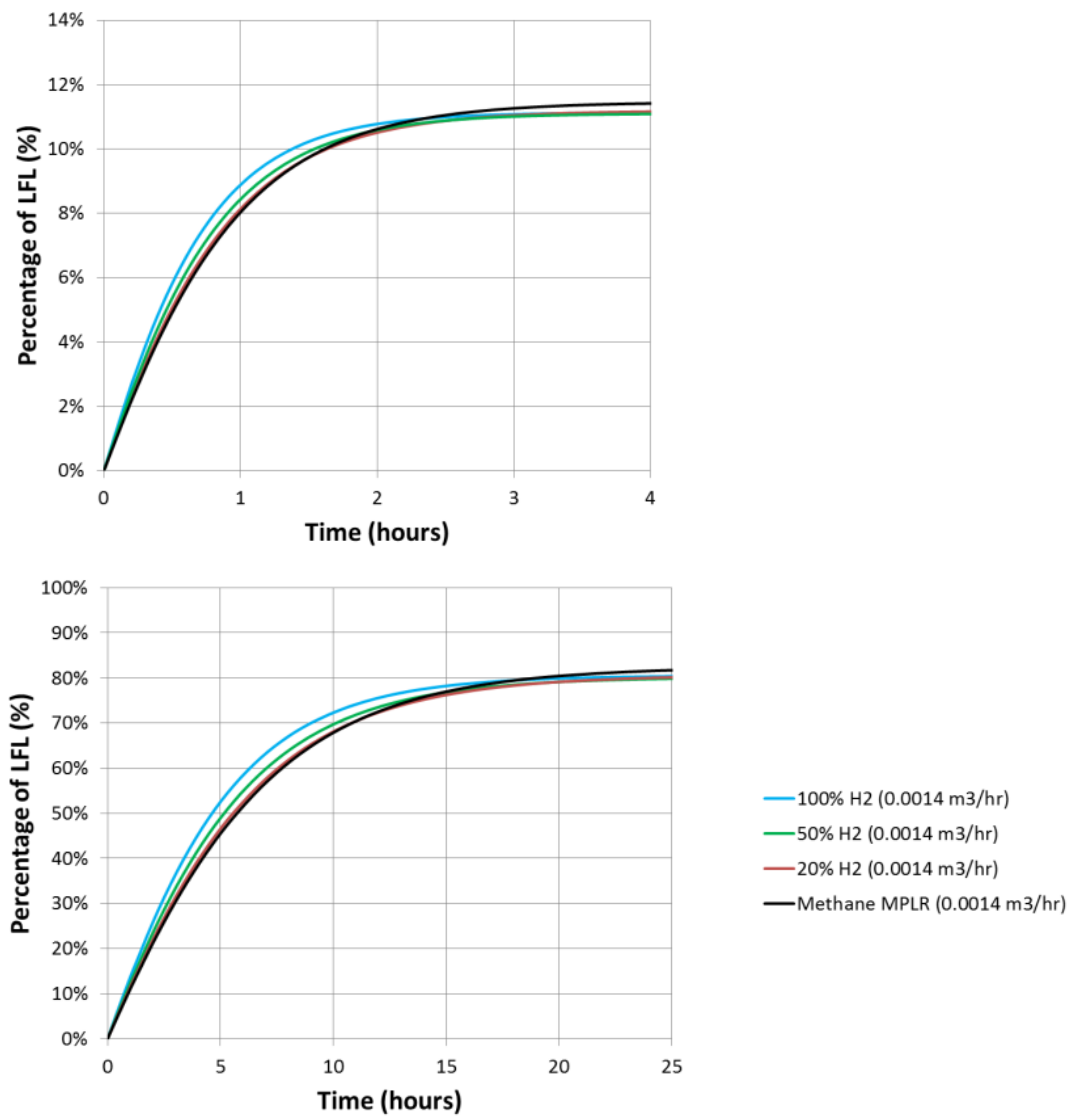


Figure 9 Predicted concentrations in a 1.0 × 1.0 × 0.5 m enclosure with ventilation openings top and bottom that are 1.0 m across and have a width of either 1 mm (top) or 0.05 mm (bottom). Four gas compositions are tested, as given in Table 3. The leak rates for all of the gases is 0.0014 m³/hr, which is currently the MPLR for natural gas in IGE/UP/1 (Scenario III).

6 CONCLUSIONS

Gas discharge and dispersion models have been analysed to assess the impact of blending hydrogen into natural gas in the UK gas transmission and distribution network. The work on gas discharge rates by Swain and Swain (1992) has been extended to consider compressible subsonic and choked releases. The results showed that these higher pressure releases behave in the same way as incompressible turbulent releases, in terms of the increase in hydrogen volume flow rate relative to methane.

Empirical correlations from Chen and Rodi (1980) have been used to assess the change in the extent of flammable clouds of hydrogen-blends relative to methane. For turbulent vertical jet releases from round holes, the analysis predicted that hydrogen-blends would produce larger flammable clouds than the equivalent methane releases. For pure hydrogen, the distance to LFL was predicted to be 3.5 times the distance for methane. For pure buoyancy-dominated plumes, flammable hydrogen clouds were predicted to extend only 1.5 times the distance of the equivalent methane clouds. These results were confirmed by comparing results to predictions from the Quadvent-2 area-classification software tool.

To demonstrate a practical application of the methods presented in this report, they were used to investigate the IGE/UP/1 procedure on leak tightness testing. Results from the analysis suggested that gas installations that have been leak tested in accordance with IGE/UP/1 under natural gas should have no increased risk of producing flammable clouds if the gas is switched to a blend of 20% hydrogen in natural gas (assuming the hole size, pressure and temperature are unchanged). IGE/UP/1 currently defines a method for calculating the MPLR volumetric flow rate for different gases in terms of energy content. If this method is used to calculate the MPLR for pure hydrogen and hydrogen blends, gas accumulation calculations showed that the resulting higher volumetric flow rates would lead to an increased risk of producing flammable clouds. It was shown that a possible solution to this issue could be to define the MPLR for pure hydrogen and hydrogen blends to be the same as the current MPLR for natural gas in volumetric terms rather than energy, i.e. 0.0014 m³/hr for new installations or existing installations with Area Type A. The gas accumulation model predicted practically identical gas concentrations in terms of percentage LEL for pure methane, hydrogen blends and pure hydrogen in that case.

Future work should consider extending the preliminary analysis presented here to instead use realistic natural gas compositions instead of pure methane. This may affect some of the results, particularly those for high-pressure releases. Work is continuing at HSE and DNV GL on the H21, H100, HyDeploy and Hy4Heat projects to further investigate gas leakage and dispersion behaviour of pure hydrogen and hydrogen blends. As part of the H21 project, leakage tests are being undertaken at the HSE Science and Research Centre in Buxton on assets that have been recovered from the UK gas network. DNV GL is also conducting experiments at Spadeadam on gas releases both above and below ground. HSE is also conducting wind-tunnel experiments to validate gas accumulation models for hydrogen blends as part of the HyDeploy-2 project, and DNV GL is conducting tests on confined gas releases within buildings for the Hy4Heat project. All of this work will contribute to the evidence base to support the safe repurposing of the gas network for hydrogen, which ultimately will help us to meet climate-change targets.

7 REFERENCES

- Birch, A.D., Brown, D.R., Dodson, M.G. and Swaffield, F., 1984. The structure and concentration decay of high pressure jets of natural gas, *Combust. Sci. and Tech.* 36, 249-261.
- Birch, A.D., Hughes, D.J., Swaffield, F., 1987. Velocity decay of high pressure jets, *Combust. Sci. and Tech.* 52, 161-171.
- Brokaw, R.S., 1968. Viscosity of gas mixtures, NASA Technical Note TN D-4496, National Aeronautics and Space Administration, Washington DC, USA. Available from <https://ntrs.nasa.gov/archive/nasa/casi.ntrs.nasa.gov/19680012255.pdf>, accessed 20 September 2019.
- BSI, 2019. Explosive atmospheres, Part 20-1: Material characteristics for gas and vapour classification – Test methods and data, BS EN 80079-20-1:2010, BSI Standards Publication, ISBN 978 0 539 12202 2.
- BSI, 2015. Explosive atmospheres, Part 10-1: Classification of areas – Explosive gas atmospheres, BS EN 60079-10-1, BSI Standards Publication, ISBN 978 0 580 96948 5.
- Chaineaux, J. and Schumann, St., 1995. Experimental study of explosions generated from the massive release of a flammable gas, as a high momentum jet, for different conditions (free or obstructed, steady or transient, jet of CH₄, C₃H₈ or H₂), 8th International Symposium on Loss Prevention and Safety Promotion in the Process Industries, Anvers, 6-9 June 1995, p317-331.
- Chen, C.J. and Rodi, W., 1980. Vertical turbulent buoyant jets: a review of experimental data, Pergamon Press Ltd, Oxford, England, ISBN 0 08 024772 5.
- Coward, H.F. and Jones, G.W., 1952. Limits of flammability of gases and vapors, US Bureau of Mines Bulletin 503. Available from <https://apps.dtic.mil/dtic/tr/fulltext/u2/701575.pdf>, accessed 20 September 2019.
- CRC, 2008. CRC Handbook of Chemistry and Physics, CRC Press, Taylor & Francis Group, ISBN 13: 978 1 4200 6679 1.
- Davidson, T.A., 1993. A simple and accurate method for calculating viscosity of gaseous mixtures, Report of Investigations 9456, US Bureau of Mines. Available from https://stacks.cdc.gov/view/cdc/10045/cdc_10045_DS1.pdf, accessed 19 September 2019.
- Ewan, B.C.R and Moodie, K., 1986. Structure and velocity measurements in underexpanded jets, *Combust. Sci. and Tech.* 45, 275-288.
- Gant, S.E., Lea, C.J., Pursell, M.R., Fletcher, J., Rattigan, W. and Thyer, A.M., 2011. Flammability of hydrocarbon and carbon dioxide mixtures: measurements and modelling, Health and Safety Laboratory Report MSU/2010/21, 2011.
- George, W.K., 1989. The self-preservation of turbulent flows and its relation to initial conditions and coherent structures, in: *Recent Advances in Turbulence*, Hemisphere, New York, 1989, pp. 39–73. Available from: http://turbulence-online.com/Publications/Journal_Papers/Papers/George89.pdf, accessed 28 October 2019.
- Harris, R.J., 1983. The investigation and control of gas explosions in buildings and heating plant, Spon Press, ISBN 978-0419132202. An updated version of this book is being prepared by DNV GL – contact Dr. Michael Acton for details (email: michael.acton@dnvgl.com).

GSMR, 1996. UK Gas Safety (Management) Regulations 1996, UK Statutory Instruments 1996, No. 551. Available from: <http://www.legislation.gov.uk/ukxi/1996/551/contents/made>, accessed 25 November 2019.

IGEM, 2005. Strength testing, tightness testing and direct purging of industrial and commercial gas installations, Utilization Procedure IGE/UP/1, Institute of Gas Engineers and Managers (IGEM), Communication 1716, August 2005.

Keagy, W.R. and Weller, A.E., 1949. A study of freely expanding inhomogeneous jets, Proceedings of the Heat Transfer and Fluid Mechanics Institute, University of California, Berkeley, USA, 22-24 June 1949. Published by the American Society of Mechanical Engineers (ASME). Referenced by <https://www.rand.org/pubs/papers/P55.html>, accessed 15 October 2019.

Keagy, W.R., Weller, A.E., Reid, W.T. and Reid, F.A., 1949. Mixing in inhomogeneous gas jets, RAND Corporation Report R-142, Santa Monica, California, February 1949. Available from <https://www.rand.org/pubs/reports/R142.html>, accessed 15 October 2019.

Kobayashi, Y., Kurokawa, A. and Hirata, M., 2007. Viscosity measurement of hydrogen-methane mixed gas for future energy systems, J. Therm. Sci. Tech. 2(2), 236-244. Available from <https://doi.org/10.1299/jtst.2.236>, accessed 19 September 2019

Kreiger, F.J., 1951. Calculation of the viscosity of gas mixtures, US Air Force Project RAND Research Memorandum RM-649, 13 July 1951, RAND Corporation, Santa Monica, California, USA. Available from https://www.rand.org/content/dam/rand/pubs/research_memoranda/2008/RM649.pdf, accessed 20 September 2019.

Lowesmith, B.J., Hankinson, G., Spataru, C. and Stobhart, M., 2009. Gas build-up in a domestic property following releases of methane/hydrogen mixtures, Int. J. Hydrogen Energy 34(14), 5932-5939. Available from: https://repository.lboro.ac.uk/articles/Gas_build-up_in_a_domestic_property_following_releases_of_methane_hydrogen_mixtures/9242582, accessed 25 November 2019.

Massey, B., 1990. Mechanics of Fluids, Chapman and Hall, London, ISBN 9780278000476.

Molkov, V., 2015. Fundamentals of Hydrogen Safety Engineering I, bookboon eBook company, ISBN 978-87-403-0226-4. Available from <https://bookboon.com/en/fundamentals-of-hydrogen-safety-engineering-i-ebook>, accessed 21 October 2019.

Ricou, F.P. and Spalding, D.B., 1961. Measurement of entrainment by axisymmetrical turbulent jets, J. Fluid Mech. 11(1), 21-32. Available from <https://doi.org/10.1017/S0022112061000834>, accessed 3 October 2019.

Reid, R.C., Reid, R.D., Prausnitz, J.M., Sherwood, T.K., 1977. The properties of gases and liquids, McGraw-Hill, 1977, ISBN 9780070517905.

Ruffin, E., Mouilleau, Y. and Chaineaux, J., 1996. Large scale characterization of the concentration field of supercritical jets of hydrogen and methane, J. Loss Prev. Process Ind. 9(4), 279-284. Available from: [https://doi.org/10.1016/0950-4230\(96\)00018-6](https://doi.org/10.1016/0950-4230(96)00018-6), accessed 30 April 2020.

Smith, M.T.E., Birch, A.D., Brown, D.R. and Fairweather, M., 1986. Studies of ignition and flame propagation in turbulent jets of natural gas, propane and a gas with a high hydrogen content, 21st Symposium (international) on Combustion, The Combustion Institute, p1403-1408.

Swain, M.R. and Swain, M.N., 1992. A comparison of H₂, CH₄ and C₃H₈ fuel leakage in residential settings, Int. J. Hydrogen Energy 17(10), 807-815. Available from: [https://doi.org/10.1016/0360-3199\(92\)90025-R](https://doi.org/10.1016/0360-3199(92)90025-R), accessed 25 November 2019.

Webber, D., 2002. On defining a safety criterion for flammable clouds. Health and Safety Laboratory report HSL/2007/30. Available from: http://www.hse.gov.uk/research/hsl_pdf/2007/hsl0730.pdf, accessed 22 November 2019.

Webber, D.M., Ivings, M.J. and Santon, R.C., 2011. Ventilation theory and dispersion modelling applied to hazardous area classification, J. Loss Prev. Process Ind. 24(5), 612-621. Available from: <https://doi.org/10.1016/j.jlp.2011.04.002>, accessed 27 November 2019.

Webber, D.M., Coldrick, S. and Ivings, S., 2020. Modelling buoyant plumes for hazardous area classification, Journal publication in preparation.

Zabetakis, M.G., 1965. Flammability characteristics of combustible gases and vapors, US Bureau of Mines Bulletin 627. Available from <https://www.osti.gov/servlets/purl/7328370/>, accessed 20 September 2019.

APPENDIX A

The book on turbulent buoyant jets by Chen and Rodi (1980) provides an excellent review of experimental data, together with useful correlations for concentration in jets and plumes (which were used earlier in this report). However, some of the equations presented in their book appear at first sight to be ambiguous or contradictory. Molkov (2015) has also noted that several papers in the literature have incorrectly written the equations for concentration in jets. The aim of this Appendix is to provide additional supporting material to help interpret the equations presented by Chen and Rodi (1980) and other papers in the literature, and to help resolve several issues.

There are two equations presented by Chen and Rodi (1980) for the decay of concentration with distance in momentum-dominated jets (on Pages 28 and 37 of their book):

$$C^* = 5 \left(\frac{\rho_0}{\rho_a} \right)^{-\frac{1}{2}} \left(\frac{x}{D} \right)^{-1} \quad (\text{A.1})$$

$$\frac{\Delta c_{cl}}{\Delta c_0} = 5.4 \left(\frac{\rho_0}{\rho_a} \right)^{\frac{1}{2}} \left(\frac{x}{D} \right)^{-1} \quad (\text{A.2})$$

There is an important difference between these two equations in relation to the density ratio (ρ_0/ρ_a), where in the first equation this ratio is raised to the power (-1/2) and in the second equation it is raised to the power (1/2). At first sight, this might appear to be a typographical error, but this is not the case, as will be explained below.

The parameter C^* is defined by Chen and Rodi (1980) in their nomenclature as a dimensionless density:

$$C^* = \frac{\rho_a - \rho_{cl}}{\rho_a - \rho_0} \quad (\text{A.3})$$

where ρ_a , ρ_0 and ρ_{cl} are, respectively, the ambient density, the source fluid density, and the centreline density (i.e. the density of the mixture of source fluid and ambient fluid on the centreline of the jet at distance x).

The density of a mixture of two fluids is the volume-fraction weighted sum of the component fluid densities, i.e.:

$$\rho_{cl} = f\rho_0 + (1 - f)\rho_a \quad (\text{A.4})$$

where f is the volume fraction of the source fluid. Substituting Equation A.4 into A.3 gives:

$$C^* = \frac{\rho_a - [f\rho_0 + (1 - f)\rho_a]}{\rho_a - \rho_0} \quad (\text{A.5})$$

which can be simplified to:

$$C^* = f \quad (\text{A.6})$$

In other words, C^* is the concentration of the source fluid, expressed as a volume fraction.

Returning to Equation A.2, it is unclear in this expression whether the terms Δc_{cl} and Δc_0 are volume fractions or mass fractions. Chen and Rodi (1980) simply referred to c as being a concentration. Equation A.2 is presented in their book beside a graph of the concentration decay in jets, which includes various experimental datasets for carbon dioxide, helium, air and smoke (see Figure A.1). To determine whether the terms Δc_{cl} and Δc_0 are mass fractions or volume fractions, the source of the experimental data plotted in their graph has been investigated.

The experimental data presented in Figure A.1 for helium and carbon dioxide (cited by Chen and Rodi as reference [44]) is a conference paper by Keagy and Weller (1949). This 70 year old conference paper is difficult to source. The RAND website¹⁶ notes that the conference paper was superseded by a report published by the same authors (Keagy *et al.*, 1949), and RAND provides a digital print of this report on their website.

The Keagy *et al.* (1949) RAND report presents two graphs for concentrations in jets of helium and carbon dioxide, consisting of model predictions and measurements (reproduced here in Figure A.2). Keagy *et al.* (1949) stated that the concentration, C , in these figures was a volume fraction. The square and round symbols in Figure A.2 are marked as concentration and velocity, respectively. However, it appears that there is a mistake and they should be the opposite way around (i.e. \blacksquare should be velocity, and \bullet should be concentration). This hypothesis is supported by the fact that symbols match the model predictions when they are the opposite way around, and the report makes no mention of this otherwise strange coincidence. Furthermore, the conference paper by Keagy and Weller (1949) (which can still be obtained from ASME for a fee) presents the symbols the opposite (i.e. correct) way around (see Figure A.3). There are also data points that appear in Keagy and Weller's graphs (Figure A.3) which are absent in the Keagy *et al.* report (Figure A.2).

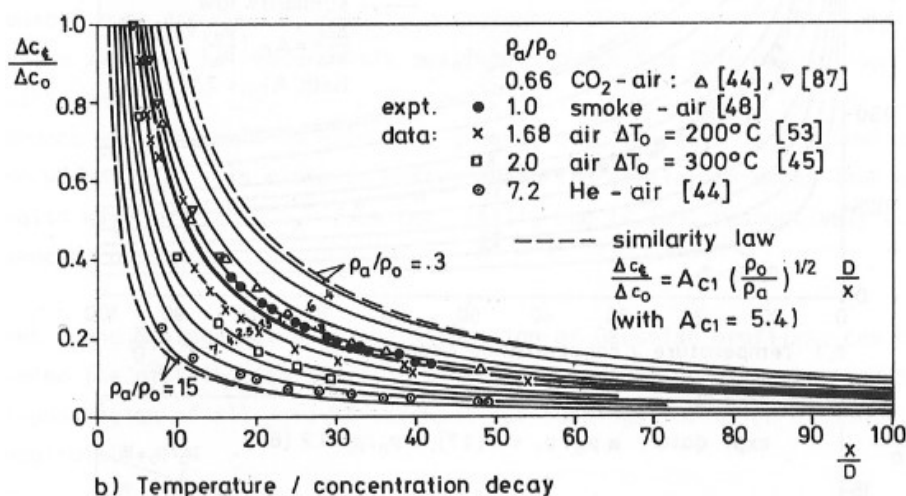
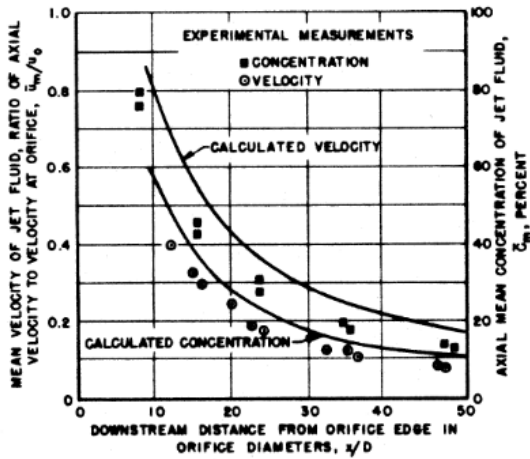
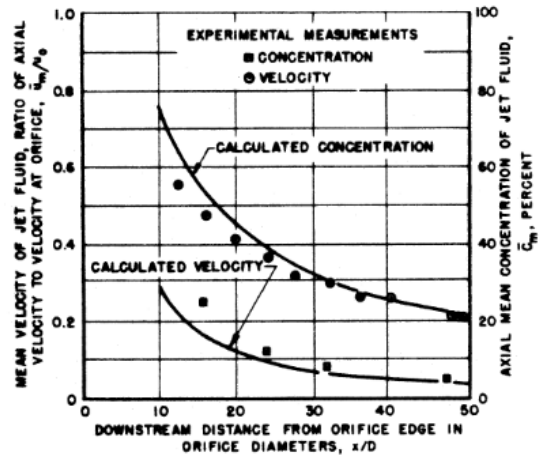


Figure A.1 Concentration (mass fraction) in turbulent round jets. Reprinted with permission from Chen and Rodi (1980).

¹⁶ <https://www.rand.org/pubs/papers/P55.html>, accessed 15 October 2019.



COMPARISON OF MEASURED AXIAL CONCENTRATION AND VELOCITY IN A JET OF CARBON DIOXIDE WITH THE CALCULATED VALUES



COMPARISON OF MEASURED AXIAL CONCENTRATION AND VELOCITY IN A JET OF HELIUM WITH THE CALCULATED VALUES

Figure A.2 Concentration (volume fraction) in jets of carbon dioxide and helium, reproduced with permission from Keagy *et al.* (1949) © RAND Corporation

Concentration data from Keagy and Weller (1949) have been digitised and converted from volume fractions to mass fractions, using the following formulae:

$$y = \frac{fM_0}{fM_0 + (1-f)M_a} \quad (\text{A.7})$$

where M_0 is the molecular weight of the source gas (either carbon dioxide $M_0 = 44$ g/mol, or helium $M_0 = 4$ g/mol) and M_a is the molecular weight of the ambient fluid (air, $M_a = 29$ g/mol). The graph of mass fraction (y) versus distance (x/D) has then been overlaid on the original graph from Chen and Rodi (1980) (see Figure A.4) to demonstrate that the two datasets are in agreement. The conclusion from the analysis of these graphs is that the concentrations presented in Chen and Rodi's data (Figure A.1) and in their Equation A.2 for the ratio $(\Delta c_{cl}/\Delta c_0)$ are mass fractions.

Molkov (2015) reached this same conclusion and he also noted that other authors, including Birch *et al.* (1984, 1987), had incorrectly written the concentration in jets as being in terms of the volume fraction, f :

$$f = 5.4 \left(\frac{\rho_a}{\rho_0} \right)^{\frac{1}{2}} \frac{D}{x} \quad (\text{A.8})$$

This equation, which Molkov (2015) stated was incorrect, is the same as Equation A.1 presented by Chen and Rodi (1980), except for the minor difference in the constant (a value of 5.4 versus 5).

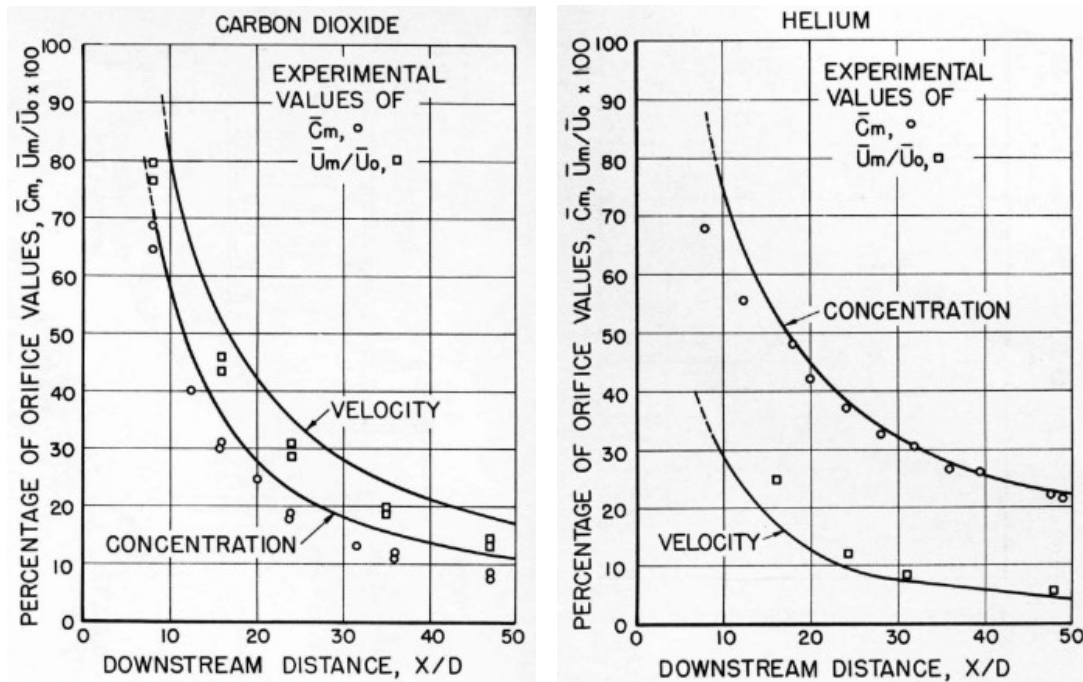


Figure A.3 Concentration (volume fraction) in jets of carbon dioxide and helium, reproduced with permission from Keagy and Weller (1949) © ASME

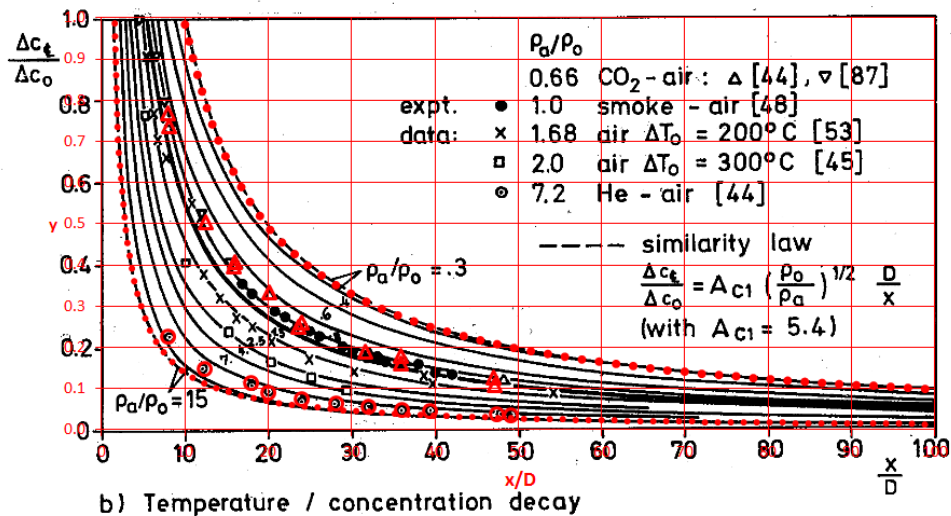


Figure A.4 Concentration (mass fraction) graph from Chen and Rodi (1980) (in black) overlaid with data from Keagy and Weller (1949) (in red)

Chen and Rodi (1980) demonstrated good agreement between measurement data and their correlation for mass fraction (Equation A.2 in Figure A.1) but did not show results in terms of the volume fraction. It is useful to make this comparison to show whether their formula for volume fraction (Equation A.1) or that of Birch *et al.* (Equation A.8) shows similarly good agreement.

To convert a mass fraction (y) into a volume fraction (f), the following equation can be used:

$$y = f \frac{\rho_0}{\rho_{cl}} \quad (\text{A.9})$$

where ρ_{cl} is the density of the mixture of source and ambient fluids on the jet centreline at the given concentration (see Equation A.4). Substituting this into Equation A.8 gives:

$$y = f \frac{\rho_0}{\rho_{cl}} = 5.4 \left(\frac{\rho_0}{\rho_a} \right)^{\frac{1}{2}} \left(\frac{x}{D} \right)^{-1} \quad (\text{A.10})$$

which can be rearranged to give:

$$f_{CR2} = 5.4 \left(\frac{\rho_{cl}}{\rho_0} \right) \left(\frac{\rho_0}{\rho_a} \right)^{\frac{1}{2}} \left(\frac{x}{D} \right)^{-1} \quad (\text{A.11})$$

Here the subscript *CR2* has been added to denote that this equation originates from second of Chen and Rodi correlations (Equation A.2), for the mass fraction.

If the centreline density is assumed to be approximately equal to the ambient density ($\rho_{cl} \approx \rho_a$), the above equation can be written:

$$f_B \approx 5.4 \left(\frac{\rho_0}{\rho_a} \right)^{-\frac{1}{2}} \left(\frac{x}{D} \right)^{-1} \quad (\text{A.12})$$

which matches the Birch *et al.* equation (Equation A.8) – hence the subscript *B* in this expression for Birch. This approximation that the centreline density is equal to the ambient density is valid in situations where the source fluid density is similar to the ambient density, or where the distances of interest are sufficiently far downstream that the concentration of the source fluid is low. To explore whether this approximation is valid for the cases of interest here, Figure A.5 shows the experimental data from Keagy and Weller (1949) in terms of the volume fraction with three sets of model predictions, using Equations A.1, A.11 and A.12.

Looking at the helium data in Figure A.5, Molkov (2015) is correct in the sense that Equation A.11 matches the experimental data, whilst the other two approximations (Equations A.1 and A.12) over-predict the concentration significantly near the source (a factor of 1.6 over-prediction at $x/D = 20$). The approximation used by Birch *et al.* (1984, 1987) (Equation A.12) is not valid in this near field region for helium.

The difference between the three models is much less significant for carbon dioxide, where all three Equations give similar results. This change in behaviour depending on the gas (helium versus carbon dioxide) is related to the difference in the density between source fluid and the ambient. For helium, the source and ambient densities are different by a factor of 7, whereas for carbon dioxide it is just a factor of 1.5.

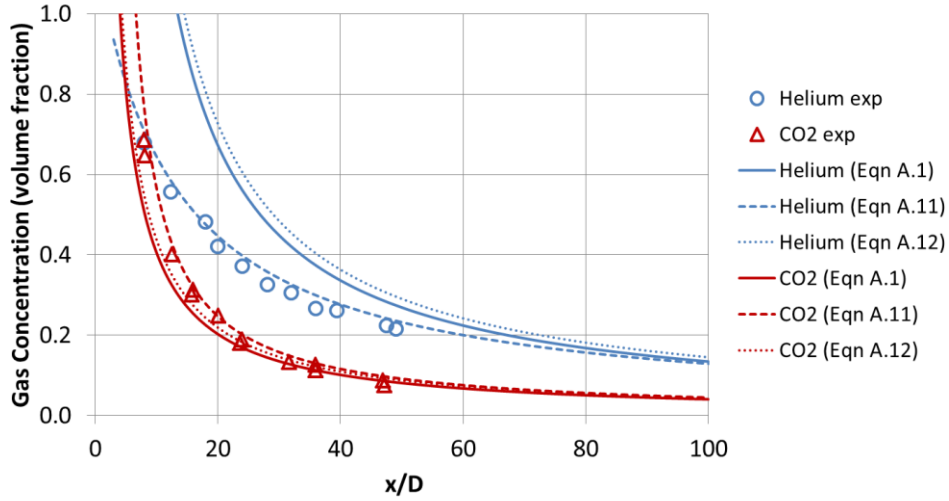


Figure A.5 Concentration (volume fraction) in jets of helium and carbon dioxide. Symbols show data from Keagy and Weller (1949). Lines show three different model predictions, using Equations A.1, A.11 and A.12.

Birch *et al.* (1984) examined jets of natural gas, which has a difference in density relative to air of a factor of approximately 1.8. In their later work, Birch *et al.* (1987) studied jets of air. Therefore, in their work, the approximation that $\rho_{mix} \approx \rho_a$ was valid.

When we consider hydrogen, the difference in density between hydrogen and air is a factor of 14. Therefore, based on the results shown in Figure A.5, the approximation $\rho_{mix} \approx \rho_a$ should not be used in the near-field. The difference in behaviour with methane and hydrogen is shown in Figure A.6.

The difference between the correlations (Equations A.1, A.11 and A.12) diminishes with distance downstream, as the jet density approaches the ambient density. If the primary interest is in assessing the distance to the LFL concentration it would appear from Figure A.6 that the correlations should give similar results, i.e. a small error. The error resulting from the approximation $\rho_{mix} \approx \rho_a$ can be assessed by equating Equations A.11 and A.12 (i.e. setting $f_{CR2} = f_B$). After some algebra, this gives:

$$\frac{x_{CR2}}{x_B} = 1 - f_{CR2} \left(1 - \frac{\rho_0}{\rho_a} \right) \quad (\text{A.13})$$

The above equation expresses the difference between the Chen and Rodi (1980) and Birch *et al.* correlations in terms of the ratio of the distances predicted by the two models (x_{CR2}/x_B) as a function of the concentration, f_{CR2} , and the density ratio, ρ_0/ρ_a . The two correlations tend to give the same predictions (a ratio of x_{CR2}/x_B approaching a value of 1) as the source fluid density tends to the ambient density ($\rho_0/\rho_a \rightarrow 1$) or as the concentration tends to zero ($f_{CR2} \rightarrow 0$).

The LFL for hydrogen is 4% v/v (i.e. $f_{CR2} = 0.04$) and the density ratio is $\rho_0/\rho_a = 2/29$. The above equation gives the result that the distance to LFL using the Chen and Rodi (1980) correlation (Equation A.11) is 1.04 times the distance to the LFL from the Birch *et al.* (1984, 1987) correlation (Equation A.12). For the distance to 50% LFL, the factor is 1.02. Further results are plotted in Figure A.7 for hydrogen and methane. Overall, for the distances commonly of interest (i.e. distance to LFL and 50% LFL), the error resulting from assuming $\rho_{mix} \approx \rho_a$ is relatively modest (an error of less than 5% in the predicted distance to LFL).

In summary, Chen and Rodi (1980) presented two equations for concentrations in jets: the first one in terms of the volume fraction (Equation A.1) and the second in terms of the mass fraction (Equation A.2). The second equation was derived from analysis of experimental data for jets of fluids with different densities and the equation matches the data well. The first equation appears to have been derived from the second equation with the simplifying assumption that the source fluid density is similar to the ambient density. A similar assumption appears to have been used by Birch *et al.* (1984, 1987). This assumption can lead to relatively large errors in predicted concentrations near to the source when the source and ambient fluid densities are very different. For example, for helium in air the error in predicted concentration is around 30% v/v helium concentration at a distance of 20 jet source diameters (a prediction of 70% v/v versus a measured concentration of 40% v/v). For fluids with similar densities to the ambient (e.g. methane or carbon dioxide in air) these errors are minor or negligible. Also, at distances far downstream (irrespective of the fluid density) the errors diminish. For hydrogen in air at a distance downstream where the concentration falls to LFL, the error in the predicted distance to the LFL is just 4% (i.e. the difference between a distance of $x = 1.00$ and 1.04). For the 50% LFL, the error in the predicted distance is 2%.

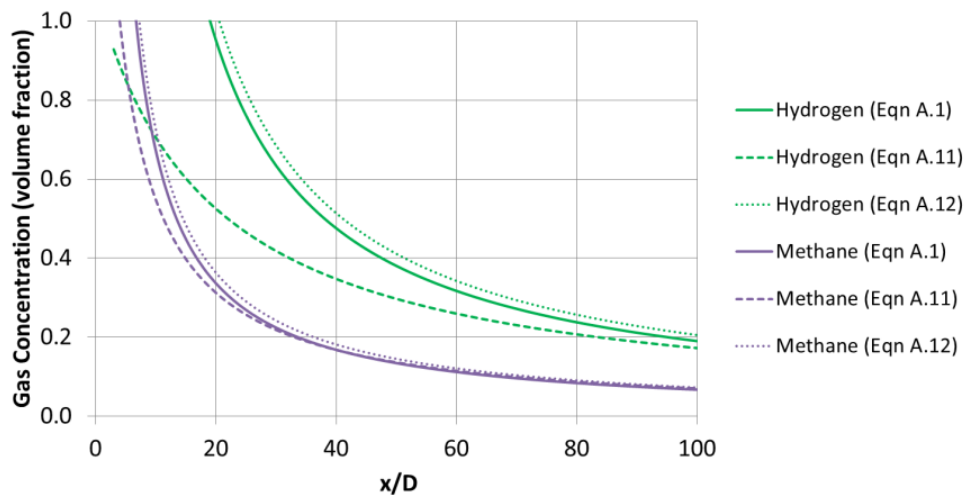


Figure A.6 Concentration (volume fraction) in jets of hydrogen and methane. Lines show three different model predictions, using Equations A.1, A.11 and A.12.

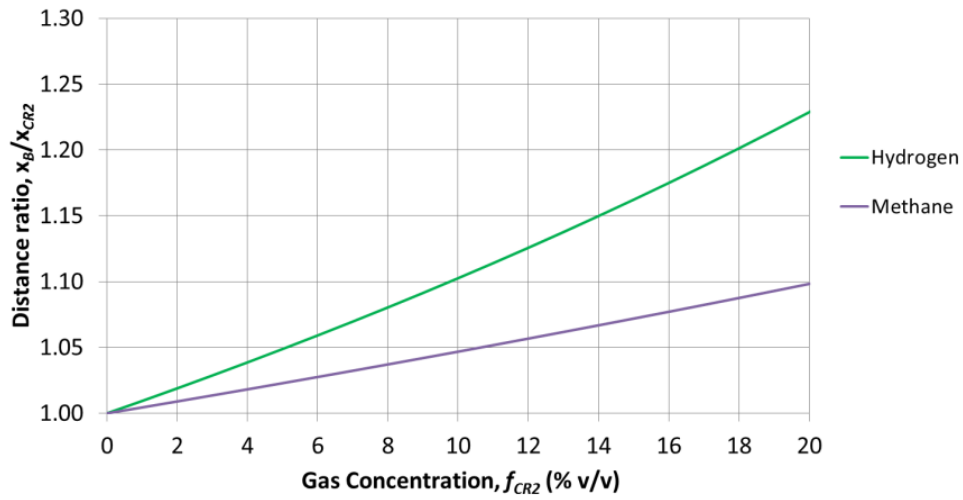


Figure A.7 Distance ratio x_B/x_{CR2} as a function of gas concentration for hydrogen and methane. This expresses the error in the predicted distance to a given concentration due to the assumption used by Birch *et al.* (1984, 1987) that the jet density is equal to the ambient density. For a gas concentration of 10% v/v, there is a 10% error in the distance for hydrogen and a 5% error in the distance for methane.

Hydrogen has the potential to be used as part of decarbonising the future energy system. Hydrogen can be used as a fuel ‘vector’ to store and transport low-carbon energy. Several UK projects are investigating the potential use of the existing natural gas transmission and distribution network to transport either hydrogen, or blends of hydrogen and natural gas, from production or storage sites to domestic or commercial appliances such as boilers, cookers, fires and ranges. Mathematical modelling is important to inform risk assessments to ensure that levels of safety for the public are maintained.

This report describes preliminary mathematical modelling of potential leaks from gas network assets such as valves and pipes when hydrogen, or hydrogen blends, are transported or used. The research considers the potential impact of leak rates and the dispersion behaviour of the gas. It uses published information from laboratory-scale experiments. The report presents a preliminary modelling case study to show how this potential impact might affect a commonly-used UK gas industry leak tightness testing procedure.

This research will be of interest to risk assessment specialists in the gas industry.